Journal of Chromatography A, 1439 (2016) 3–25

Contents lists available at ScienceDirect

Journal of Chromatography A

journal homepage: www.elsevier.com/locate/chroma

Review article

Hybrid ion mobility and mass spectrometry as a separation tool

Michael A. Ewing*, Matthew S. Glover, David E. Clemmer

Department of Chemistry, Indiana University, Bloomington, IN 47405, United States

ARTICLE INFO

Article history:
Received 2 July 2015
Received in revised form 5 October 2015
Accepted 21 October 2015
Available online 10 November 2015

Keywords:
Ion mobility spectrometry
Mass spectrometry

ABSTRACT

Ion mobility spectrometry (IMS) coupled to mass spectrometry (MS) has seen spectacular growth over the last two decades. Increasing IMS sensitivity and capacity with improvements in MS instrumentation have driven this growth. As a result, a diverse new set of techniques for separating ions by their mobility have arisen, each with characteristics that make them favorable for some experiments and some mass spectrometers. Ion mobility techniques can be broken down into dispersive and selective techniques based upon whether they pass through all mobilities for later analysis by mass spectrometry or select ions by mobility or a related characteristic. How ion mobility techniques fit within a more complicated separation including mass spectrometry and other techniques such as liquid chromatography is of fundamental interest to separations scientists. In this review we explore the multitude of ion mobility techniques hybridized to different mass spectrometers, detailing current challenges and opportunities for each ion mobility technique and for what experiments one technique might be chosen over another. The underlying principles of ion mobility separations, including: considerations regarding separation capabilities, ion transmission, signal intensity and sensitivity, and the impact that the separation has upon the ion structure (i.e., the possibility of configurational changes due to ion heating) are discussed.

Contents

* Corresponding author.
E-mail address: miewing@indiana.edu (M.A. Ewing).

http://dx.doi.org/10.1016/j.chroma.2015.10.080
0021-9673/

1. Introduction

Ion mobility spectrometry (IMS), also at times known as plasma chromatography [1] and ion chromatography [2–4], was originally developed as a tool for the separation of ions of interest by a linear field applied to a drift tube containing a buffer gas [5]. The buffer gas impedes ion progress, counteracting the acceleration of the ions in applied electric fields. As a result, ions travel at a terminal velocity proportional to the inverse of their collision cross section (CCS), a parameter that describes the orientational average of collision rate, in a manner analogous to the terminal velocity of a skydiver depending on the skydiver's shape. The CCS is smaller for more compact (more spherical) molecules than for more extended ones (e.g., planar structures, extended chains, helices, etc.) and thus yields insight into the overall shape. For example, this insight has been used to determine that carbon clusters exist as chains, rings, planar graphite-like sheets, and fullerenes depending on the number of atoms in the clusters [2,6–11]. In the seemingly distant field of structural biology, the approach has been used to determine the topology of an intact ATPase as well as conditions that favor the attachment and detachment of different components and the dynamics of those components [12,13].

In addition to identifying the shape of a given ion, ion mobility can be used to separate mixtures containing isobaric (and thus isomeric) ions by shape [14]. In particular, the separation time of drift tube ion mobility spectrometry (typically milliseconds) fits well between that of liquid separation techniques such as liquid chromatography and capillary electrophoresis, with typical separation times of seconds to minutes, and mass spectrometry (MS), which often operates on the microsecond time scale. Because of the unique separation phenomenon, the ability to glean structural insights from the CCS, and the relative time scale of drift tube separations and mass spectrometric analyses, coupling IMS with MS can be used to influence a range of useful separation parameters, yielding: enhanced peak capacity, reduction in total analysis time, reduction of chemical noise, decreased detection limit, and valuable analyte structural information.

Since the dawn of the millennium, IMS has emerged as a powerful means of enhancing the separation of components found in complex mixtures – that is, these methods are especially valuable when coupled to other separation techniques such as mass spectrometry and liquid chromatography [15–26]. The extra dimension of separation has enhanced the number of peptides identified in proteomics studies [18,27–29] and enabled metabolomics studies [26,30,31]. The ability to dissociate ions in parallel [32–38] has promised to advance the identification of proteins in the field of proteomics [21,23,27,39]. The ability to distinguish isomers of glycans presents a novel diagnostic tool for disease progression [40–42]. And the ability to predict CCS from peptide sequence can enhance the confidence in peptide assignment [43–45]. Many other fields have benefited from the increased separation powers available when ion mobility spectrometry is coupled to mass spectrometry including petroleomics [46,47] and polymer separation [48–51].

One of the most powerful aspects of this technology is that it can provide information about the three-dimensional structures of ions – where few options for determining structure exist. While the determination of cross-section from the conformation of the molecule and the relation to diffusion constants was first described by Mack in 1925 using beeswax [52], it was not regularly applied to IMS for quite some time. This aspect of these measurements was revolutionized in the early 1990s by the Bowers and Jarrold groups when they compared measured mobilities or cross sections with values that were calculated for trial geometries generated by computations [2–4,6,53–58]. While this modern use of the approach is now widely used, from its inception, IMS was used to infer the structure and composition of analytes, such as in the separation of the charge states of cytochrome *c* shown in Fig. 1 [59].

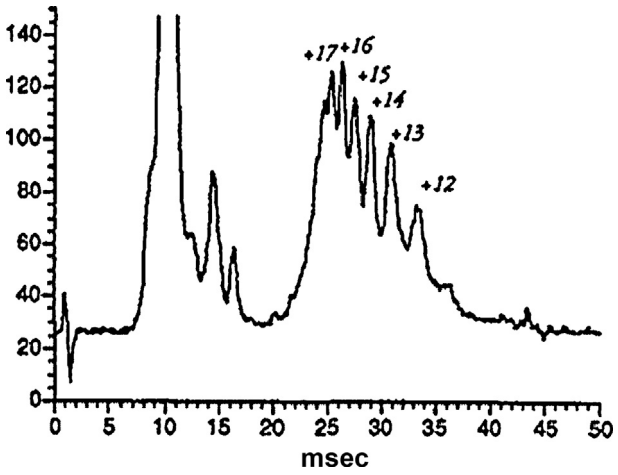

Fig. 1. ESI-IMS spectrum of cytochrome *c* showing separation of different charge states by IMS.

Adapted with permission from D. Wittmer, B.K. Luckenbill, H.H. Hill, Y.H. Chen, Electrospray-ionization ion mobility spectrometry, Anal. Chem., 66 (1994) 2348–2355. Copyright 1994 American Chemical Society [59].

Groups at Bell Labs [60–62] and Georgia Tech [63,64] first coupled ion mobility spectrometry with mass spectrometry over 50 years ago but the technique saw limited analytical use. Much of the earliest instrumentation in this field was dependent upon scanning a dual gate ion mobility setup [60,62–64] to determine the mobility of ions by only gating out those ions that traversed the drift tube in a predetermined time, and then scanning the delay between the entrance and exit gates. IMS coupled to orthogonal time-of-flight (TOF) MS was first developed by McAfee et al. [60]; on a similar instrument Young et al. [61] was able to generate multiple pulses into the TOFMS flight tube per drift spectrum but still required scanning the pulses into the TOFMS flight tube to obtain a full spectrum [61]. Full spectral coverage, and the accompanying increase in throughput, was only obtained with the development of nested orthogonal TOFMS [65], whereby ions were pulsed into a TOFMS across the entire time course of the drift separation in order to obtain the mass and mobility for (conceptually) all ions in a single mobility separation as described in more detail below. The dramatic increase in throughput and sensitivity make this a key step delineating older techniques used for analyzing simple mixtures from newer experiments wherein complex mixtures can be analyzed. Demonstrations of high signal [18] with the new advances in instrumentation drove further advances in instrumentation as the requirements of different applications determined what aspects of the separation were preferable.

In this review we examine a range of IMS–MS-based experiments – primarily focused on enhancing separations of complex mixtures. Taking into account the wide range of needs of different experiments, we consider what factors might lead a user to prefer some techniques available for coupled mobility and mass separations. To better understand the distinctions between techniques, we will examine each technique individually, focusing on fundamentals of the technique, the separation capacity, the limits of detection, the relationship between the instrumentally measured mobility and the gas-phase structure, and the causes and effects of heating of ions within the instruments provided. For each technique we also provide an example experimental dataset and a very brief discussion of the data that is intended to familiarize the reader with how data from hybrid IMS–MS instruments is typically displayed. For a detailed understanding of each dataset that is shown, the interested reader will need to examine the original publication.

Since the development of nested drift tube (DT) IMS–MS, numerous other ion mobility separation techniques have matured or are under development. We will examine them according to their order of development within two broad classes. The first class, dispersive or nested techniques, corresponds to separations with complete spectral coverage in a single separation. Among the dispersive techniques are dispersive DTIMS [65], traveling wave ion mobility spectrometry (TWIMS) [66,67], and trapped ion mobility spectrometry (TIMS) [68,69]. The second class, selective or scanning techniques, transmit ions of a selected mobility (or related characteristic of the ion), requiring scanning the selection characteristic to obtain a full spectrum of all ions. Selective techniques discussed herein are selective DTIMS [5], differential mobility analysis (DMA) [70–74], field asymmetric waveform ion mobility spectrometry (FAIMS) also called differential mobility spectrometry (DMS) [75,76], overtone mobility spectrometry (OMS) [77,78], circular ion mobility spectrometers [79], and transversal modulation ion mobility spectrometry (TM-IMS) [80].

1.1. Separating ions based on differences in gas-phase structure

Ion mobility separations are based on differences in ion structures (or cross sections) and charge states [81]. The latter is straightforward and is determined by the excess charge on each species. Ion cross sections are related to the average shapes of the ion, which in effect determines the collision rate with the buffer gas [81]. More compact conformations undergo fewer collisions with the buffer gas than do more open (or elongated structures). Thus, compact species with small collision cross sections have higher mobilities than do more open forms of the ion.

To determine the experimental CCS of an ion, the mobility, $K = v/E$, must be determined: where K is the proportion between the speed an ion moves, v, and the electric field to which it is subjected, E [81]. Mobilities of ions were first observed and measured in the Cavendish laboratory by Rutherford [82] and Zeleny [83]. This laboratory was overseen by J.J. Thomson who was at the same time discovering the electron [84] in a very similar experiment where he was examining the negatively charged particles from a cathode ray source. Rutherford and Zeleny, known more for his later work on spraying fluid from a capillary at voltage, worked on the ions formed from X-rays and while Rutherford first determined ion velocities, he saw no difference when independently measuring the velocities of positively charged and negatively charged ions. Zeleny measured the ratios of the different velocities of the negatively and positively charged ions within his instrument, obtaining ratios of mobilities that distinguished the ions in methods that bear a strong resemblance to modern DTIMS and DMA instruments [83]. These discoveries significantly advanced our understanding of the mobility of ions in gases.

Because the mobility depends on the temperature and pressure of the measurement, a reduced mobility, K_0 which has been normalized to standard temperature and pressure, is typically reported. In low electric fields, the Nernst–Townsend–Einstein relation [1,81] relates the mobility and the diffusion coefficient. The diffusion coefficient or mobility can be used to derive a CCS for an ion, the net effect for a linear drift tube is Eq. (1), the Mason–Schamp equation [1,81],

$$\Omega = \frac{ze}{16}\left(\frac{18\pi}{k_b T}\right)^{1/2}\left(\frac{1}{m_I}+\frac{1}{m_B}\right)^{1/2}\frac{tE}{L}\frac{1}{N} \quad (1)$$

where L is the length of the drift tube, t is the drift time, k_b is the Boltzmann constant, T is the temperature, m_I is the mass of the ion, m_B is the mass of the buffer gas molecules, and N is the number density of the buffer gas at the temperature and pressure of the experiment.

To infer a structure from a mobility, molecular modeling is typically combined with a CCS estimating algorithm such as the projection approximation [2,52,53], exact hard-sphere scattering [55], trajectory method [56,57], projection superposition approximation [85–88], or scattering on electron density isosurfaces [89–91]. One important factor to note is that CCS values will change in different gasses, and while this is often approximately predictable, it is important to measure ions in different buffer gasses for the most accurate CCS values [92–98]. Additionally it should be noted that the Mason–Schamp equation is exact only in the limit of zero field as it is the truncation of a power series; electric fields where the Mason–Schamp is accurate are typically referred to as the low-field regime. While resolving powers of 10–100 are common [4,46,69,99–106], measured mobilities and CCS can be quite precise, with percent relative deviations between measurements often between ~0.1% and 2% [96,106–109]. Keeping in mind this difference between accuracy and precision, care must be taken not to over-interpret CCS values, despite their utility in comparing amongst the myriad of techniques presented herein.

One of the most important considerations when studying the gas-phase structure of ions, especially in attempts to relate the gas-phase structure back to the original solution-phase structure, is the heating of ions from ionization to detection. There is evidence that some ions retain some information of their original solution structure [110–119]; in the case of native MS often the gross structure, such as the topology of a protein complex, is retained [114], yet there are many cases where the structure clearly changes in transition from solution to analysis [115,120–123]. The desolvation of ions results in evaporative cooling that locks some structures into place at some point in the electrospray ionization process [124] such that the lack of solvent may impede structural rearrangement; the amount of heating necessary to overcome the barriers to rearrangement is different for every ion with larger ions exhibiting less heating due to inelastic collisions and thus more able to handle equal electric fields [81]. While the dominant effect of heating ions is often in interface regions, especially the region where desolvation occurs [113,124–126], separation by ion mobility occurs in an electric field and can also lead to heating of the ions [81]. In the gas-phase, temperature is typically viewed as proportional to the square of the velocity of the particles being measured. In ion mobility experiments, ions are directed by the electric field, having a higher root mean square velocity in the direction of the electric field than orthogonal to it. Since the velocity is not equal in all directions, more complex theories of temperature must be used [81] but at higher electric fields, the internal energy of the ions can be increased, potentially resulting in changes in conformation [81].

Typically the mobility of an ion (and implicitly its structure) does not significantly change in the low-field regime, a regime where the electric field, E, relative to the pressure, p, (or number density of gas, N) is low, often below ~0.1–10 Td [81,95]. The cutoff between high- and low-field regimes is both highly variable between species and gradual for many ions, with the mobility slowly changing as the electric field changes [81]. As ions heat up, they often start to unfold and change structure, although changes in mobility can also be due to the changes in the energy and momentum transfer of collisions [81]. This ion temperature affects the accuracy of the CCS information and the relevance of the CCS to the solution structure. Lower temperature experiments, including those done in cryogenic drift tubes, are often more useful for relating the structural information in the gas-phase back to the solution structures [127–131]. On the other hand, high temperature experiments [113] (or long trap times before analysis [132]) can be used to anneal distinct conformations of a single species into fewer peaks with narrow peak widths, depending on the analytes of interest and their rate of conversion [133].

2. Instrumentation and techniques

Two fundamental figures of merit are important for ion mobility techniques, the limit of detection and the separation capacity. The limit of detection (LOD) can vary wildly within a technique and between analytes and thus we will typically describe general improvements on signal transmission rather than specifics LODs. Separation capacity on the other hand is best described by peak capacity. As noted in Eq. (1), there is a correlation between CCS, and therefore ion mobility and drift time, and m/z. Because of this, the peak capacity is not strictly the multiplication of the peak capacities of IMS and MS but instead must account for the correlation between CCS and m/z and deviations from that [134]. The correlation is dependent on the molecular-class (or family of structural types), as can be seen when different compounds cluster in slightly offset portions of the full spectrum [106,135]. A definition of peak capacity is nuanced because one needs to understand how many features can be resolved at a specific m/z and this may change with m/z; thus resolving powers are typically reported.

Resolving power describes the width of a peak relative to its location in the spectrum and typically changes only slightly between different species of the same charge state on the same instrument. Because CCS, mobility, and drift time correlate reasonably well for all low-field techniques, resolving power is a reasonable but coarse benchmark for comparison between the current state of most instruments and techniques, with caveats for each technique described within the corresponding technique. There is significant variation in reported resolving powers between techniques, with the resolving power increasing with charge on the analyte. Typical resolving powers range from ~5 to 60 for low resolution instruments [4,46,69,99–104] and up to 200–1000 [136–140] for the highest reported resolving powers, depending on the technique of interest. For traditional drift tube ion mobility spectrometry (DTIMS), resolving power can be approximated from the ratio of the drift time to the full width at half-maximum of the peak as in Eq. (2) [1],

$$R \equiv \frac{t}{\Delta t} = \left(\frac{zeEL}{16k_bT\ln 2}\right)^{1/2} \quad (2)$$

2.1. Dispersive (nested) ion mobility techniques coupled to mass spectrometry

Stand-alone ion mobility spectrometers are often run with continuous detectors that disperse signal across temporally distinct bins at all (analyzed) drift times rather than selecting ions at the end of the drift tube before detection. To couple with mass spectrometry this mode of operation becomes more difficult because the mass spectrometric analysis must be completed before the next bin of drift times are analyzed, in a mode denoted nested. Dispersive ion mobility separations analyze all injected ions in one batch, eliminating losses due to ions not being of the selected mobility, and thus have a clear advantage over selective techniques when high throughput and maximum total signal is desired. Additionally, in a mode first described as parallel fragmentation [20,32,36–38] and now also incorporated within HDMS^E [141], ion mobility techniques allow for fragmentation after mobility separation and before mass analysis, such that parent and fragment ions are aligned in drift tube for easy assignment. With nested techniques, this parallel fragmentation allows for the accumulation of potentially tens of thousands of fragment spectra very quickly [27]. With proper ion optics, nested ion mobility spectrometry–mass spectrometry can be conceivably performed with any mode of mass analysis [65], but the ease of coupling with TOF mass analysis led to the development of DTIMS as the first nested IMS–MS technique [65]. Two other nested modes have since been developed, based around TWIMS [66,67] and TIMS [68,69].

All nested hybrids of ion mobility spectrometry and mass spectrometry share similar ideal characteristics. After generation, ions must be accumulated before entering into the mobility separation device in which they are separated, after separation they are injected into a mass analyzer. In the ideal, losses in transfer between each step would be minimized, accumulation would show minimal loss no matter the length of time, and mass or CCS biases would be nonexistent. In practice all of these difficulties occur to varying degrees based upon the specific geometry and potentials applied and should be considered with care when examining instruments rather than techniques.

2.1.1. Nested drift tube ion mobility spectrometry–time of flight mass spectrometry

By developing a method to inject ions into an orthogonal TOFMS at a rate proportional to their egress from the drift tube, Clemmer and coworkers developed the first fully nested IMS–MS technique [65]. In the instrument schematic shown in Fig. 2, ion optics after the drift tube set the velocity of ions such that ions traverse approximately the length of the orthogonal TOF injection window, injecting (ideally) all of the ions that exit the drift tube into the TOFMS. The time from the injection of ions into the flight tube until impact on the detector is measured and converted to m/z while the time from the pulse of the drift tube entrance gate until the TOF pulse is the drift time, also called the arrival time in some manuscripts. Because the flight time is typically in microseconds and the drift time is typically in milliseconds, this results in a nested two-dimensional spectrum. The bin size in the drift time is the periodicity of the TOF pulser; within this bin size no differences in drift times are distinguishable. Thus there is a small loss in potential resolving power in the mobility (drift time) dimension (compared to a continuous direct detector without mass analyzer) at the gain of significant resolving power in the new m/z dimension. In practice the loss of resolving power is negligible as typical resolving powers are less than 300 [136] in the best linear drift tubes to date and more bins (ToF pulses) are applied than the resolving power of the instrument [142].

Early experiments demonstrated the wide range of possible uses for this technology; examples chosen from this long list of experiments show the use of IMS–MS for the separation and analysis of components of a tryptic digest as shown in Fig. 3 [143], and the separation of different classes of compounds as shown in Fig. 4 [144]. While nested DTIMS–TOFMS drastically reduced the loss in signal from the duty cycle of the drift tube exit gate within a scan, losses due to the duty cycle of the drift tube entrance gate were still significant [65]. A major development in reducing ion losses at the drift tube entrance gate was the incorporation of a trap before injection into the drift tube. Large increases were seen going from injection of a continuous stream to a Paul trap [145], then to a linear ion trap [18], and more recently to ion funnel traps [21,23,146–149]. The last step provided trapping at higher pressures (~1–10 Torr) and thus alleviated ion losses going from a lower pressure regime (mTorr) to a higher pressure regime (Torr), a pressure gradient more commonly seen in the instruments with an ion trap prior to the drift tube. Another major loss of signal was found to be the radial diffusion of the ion cloud beyond the focusing ability at the rear of the drift tube. Again ion funnels in the middle of and at the back of the drift tube maximized transmission of ions [142,146]. Recent developments in instrumentation of DTIMS–MS have focused on eliminating signal loss by using radio frequency (rf) confinement or an equivalent DC confinement more efficiently and even throughout the entire length of the drift tube [103,148,150–160]. This allows for longer drift tubes with the same signal, and longer drift tubes can obtain higher resolving powers

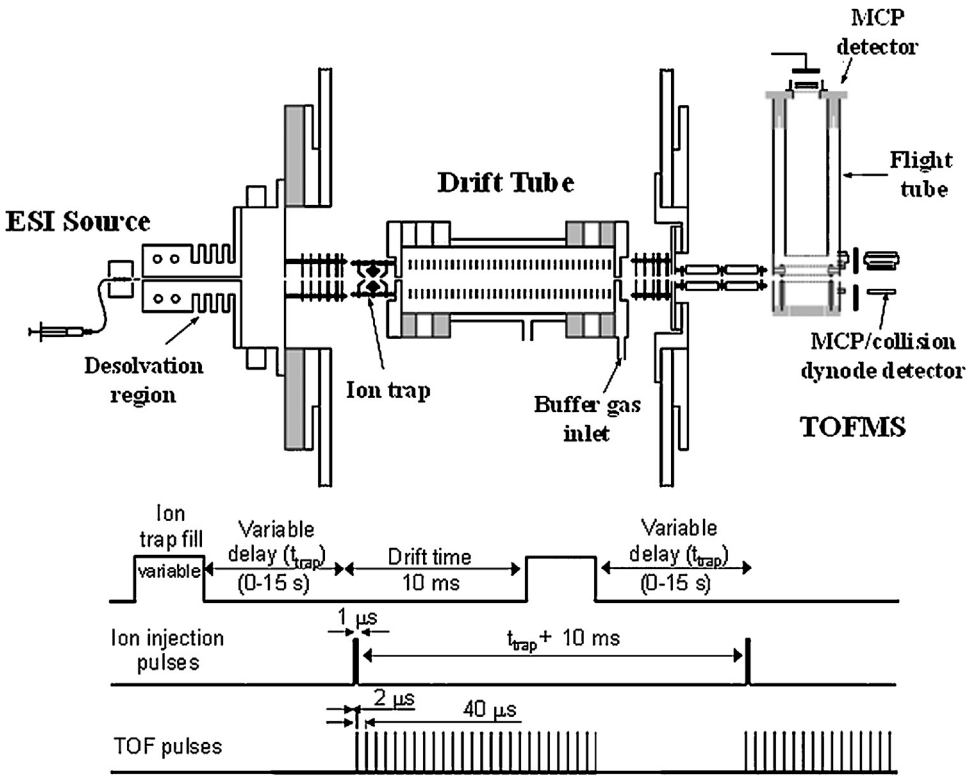

Fig. 2. Method of nested ion mobility spectrometry–time of flight mass spectrometry (IMS–TOFMS) with an orthogonal TOFMS. Ions enter from an ion source on the left and are trapped before being injected into the drift tube. Ions separate under the electric field in the drift tube before entering the orthogonal acceleration region and being pulsed into the TOF sequentially such that in theory all ions should reach the TOF detector. Improvements in electronics enabled the pulsing of all ions as they exited the drift tube, obtaining full coverage of the spectrum without the need for scanning the timing of a selective exit gate across length of the full spectrum, and thus increasing the signal of ion mobility coupled to mass spectrometry.

Reprinted with permission from S.C. Henderson, S.J. Valentine, A.E. Counterman, D.E. Clemmer, ESI/ion trap/ion mobility/time-of-flight mass spectrometry for rapid and sensitive analysis of biomolecular mixtures, Anal. Chem., 71 (1999) 291–301. Copyright 1999 American Chemical Society [143].

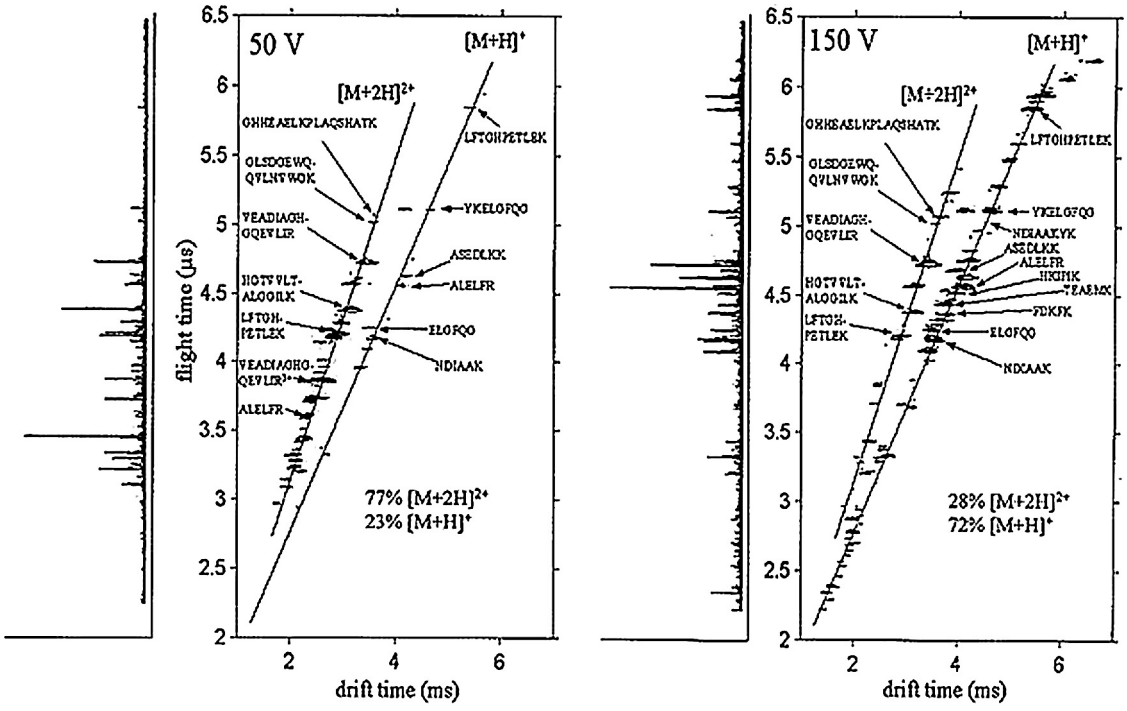

Fig. 3. Separation of a mixture of peptides from a tryptic digest of myoglobin. Source conditions have a significant effect on not just conformations but also peptide intensity, with higher voltages leading to more singly charged peptides.

Reprinted with permission from S.C. Henderson, S.J. Valentine, A.E. Counterman, D.E. Clemmer, ESI/ion trap/ion mobility/time-of-flight mass spectrometry for rapid and sensitive analysis of biomolecular mixtures, Anal. Chem., 71 (1999) 291–301. Copyright 1999 American Chemical Society [143].

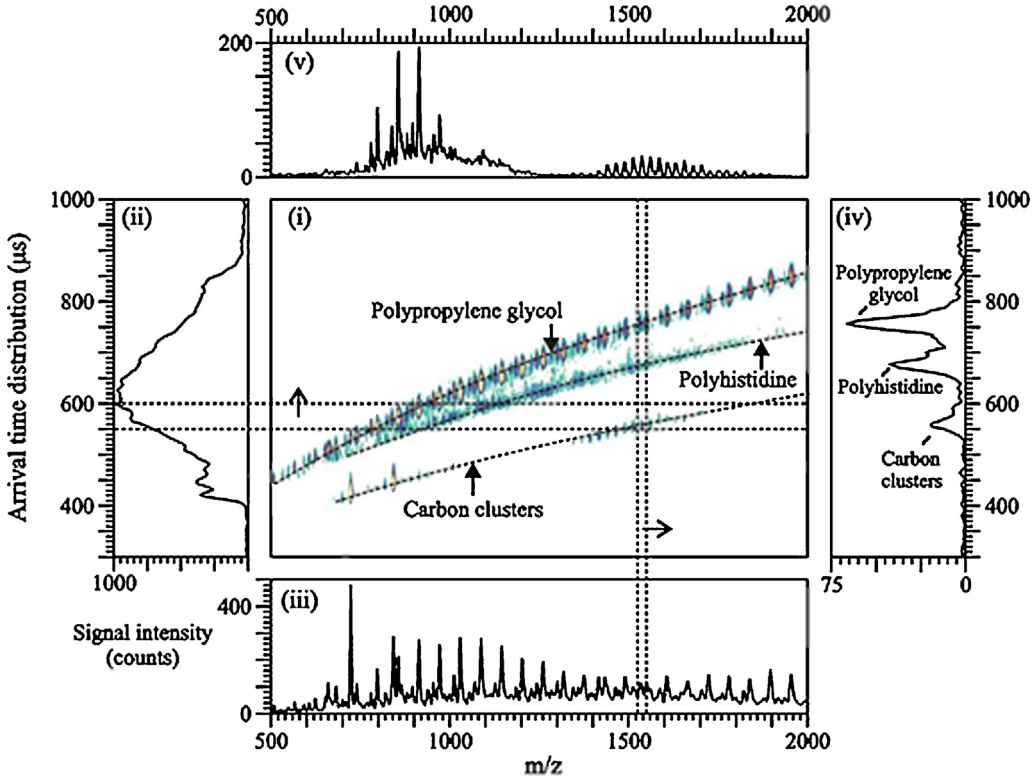

Fig. 4. (i) Two-dimensional IMS–MS spectrum showing the separation of different classes of compounds, carbon clusters, polyhistidine, and polypropylene glycol. Summed mass and mobility spectra are shown on the left (ii) and bottom (iii) of the two-dimensional spectrum. A vertical pair of dashed lines is used to delineate the portion of the spectrum summed together (between the dashed lines) to obtain the mobility distribution shown on the right (iv). A horizontal pair of dashed lines is used to delineate the mass spectrum shown on the top (v).

Reprinted from International Journal of Mass Spectrometry, 240, John A. McLean, Brandon T. Ruotolo, Kent J. Gillig, David H. Russell, 301–315, 2005, with permission from Elsevier [144].

while still yielding relevant CCS values by utilizing the low-field regime. The increasing sensitivity of DTIMS–MS instruments has made a wide range of separations desirable [143,144]. Ever more complex samples are being analyzed although typically in the same format as shown in Figs. 3 and 4, with drift time and m/z as two separate axes, color or intensity of shading denoting the intensity of peaks for an overall spectrum, and integrated mass and drift spectra from the entire data set or from selected ranges of m/z and drift time taken as needed to fully explore the data set and demonstrate interesting features.

An interesting advance in nested IMS–MS came in using relatively empty portions of the spectrum through parallel fragmentation [32–38]. Collisionally induced dissociation after ions exit the drift tube results in fragments at the same drift time as the parent but over a wide range of m/z such that fragments are often outside the band of components separated by ion mobility spectrometry [32]. The alignment of drift time enables association of fragments together with the parent ion as shown in Fig. 5. Dissociation can also be employed at the beginning of the drift tube to separate fragment ions by shape [161]. The unfolding of ions can be investigated upon the deposition of collisional energy [122,162,163], yielding energetics about various gas-phase conformations [164].

Most DTIMS–MS experiments are operated in the low-field regime for maximum structural information, but higher fields lead to increased resolving power as seen in Eq. (2). When it is purely the separation capabilities of IMS that are desired, the electric field should be optimized for the experiment at hand, but it is typical to use electric fields safely in the low-field regime when structural information is desired. Care must be taken with the latter type of experiments to ensure that the heating does not modify the mobility and CCS of each measured species in ways that contradict the validity of the experiments. At very high electric fields, especially for lower pressures in the drift tube, electrical breakdown can become a problem in accordance with Paschen's Law.

Resolving powers of DTIMS–MS instruments range up to ~250 [14] but vary significantly from instrument to instrument and typical resolving powers are often ~60–80 [106], especially in the range of pressures more common in highly sensitive instruments. Because of the wide range of instruments available, we note here only limited examples as any desirable resolving power under 250 can be found and will be dependent upon the molecular system being analyzed. As one of the first techniques developed, and the dominant coupled IMS–MS technique in the literature, we reference all other techniques to nested DTIMS–MS for comparison. Since the original development of DTIMS–MS, a number of commercially available instruments have been developed containing this coupling including those by TOFWERK, Excellims, and Agilent, democratizing the field.

2.1.2. Traveling wave ion mobility spectrometry–mass spectrometry

A similar nested ion mobility technique known as TWIMS was commercialized a decade ago by the Waters Corporation in the Synapt line of instruments [66,67,105,165]. This high performance instrument has significantly advanced the field of ion mobility spectrometry–mass spectrometry through its versatility and widespread availability. TWIMS uses a stacked ring ion guide (SRIG), which operates effectively as a drift tube, but with a dynamic application of electric field to separate the ions. Rather

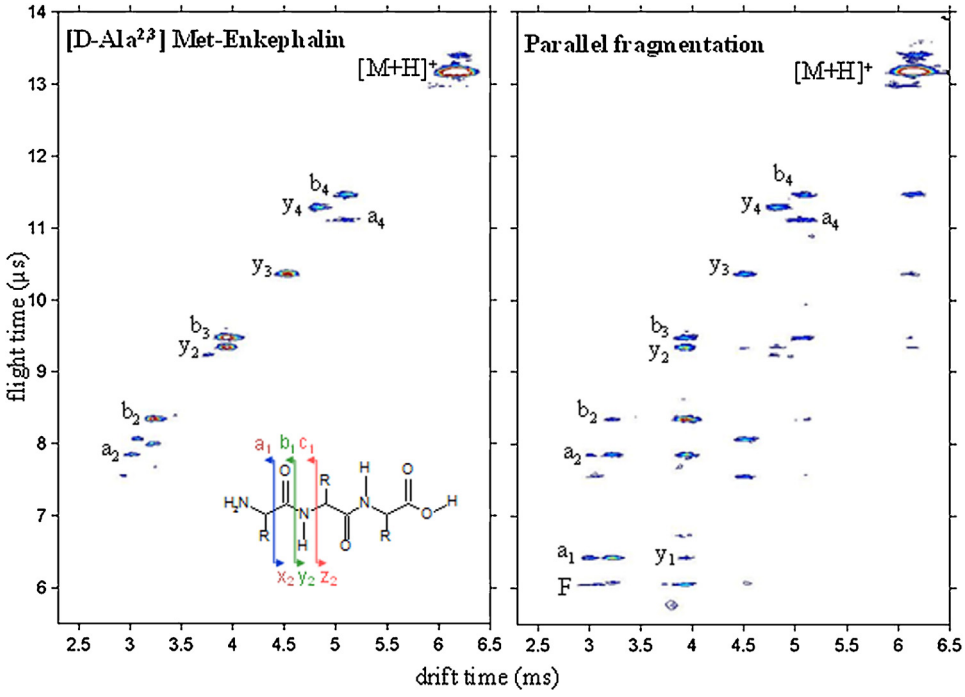

Fig. 5. Heat maps of IMS–MS (left) and IMS–MS/MS (right) spectra of [D-Ala^{2,3}] Met-Enkephalin. [D-Ala^{2,3}] Met-Enkephalin is fragmented before entry into the drift tube in the left spectrum demonstrating separation of fragment ions. Fragmentation of the mobility-separated fragments is performed after mobility separation showing temporal alignment in the drift spectrum but separation of fragments by the time-of-flight mass analyzer. Fragments formed before ion mobility fall along a band of correlated drift times and flight times. Fragmentation at the rear of the drift tube uses portions of the spectra previously devoid of peaks and leads to assignment of fragment ions to parent ions.

Reprinted with permission from C.S. Hoaglund-Hyzer, J.W. Li, D.E. Clemmer, Mobility labeling for parallel CID of ion mixtures, Anal. Chem., 72 (2000) 2737–2740. Copyright 2000 American Chemical Society [32].

than a linear electric field through the full length of the SRIG, TWIMS uses a traveling wave of electric potential that pushes ions along similar to a surfer as shown in Fig. 6. In the ideal case, a wave moves ions incrementally toward the detector before passing the ion, whereupon ions slow down before being picked up by the next wave and moved incrementally forward again. The mobility of the ion determines how often a wave passes the ion and thus how many waves are required for an ion to transit the SRIG [66,166]. Similar to many DTIMS instruments currently in use or development, the SRIG also uses radio frequency-confinement to eliminate losses of ions due to radial diffusion [66,67].

Other than this method of propagation within the drift tube, TWIMS instruments typically operate identical to nested IMS–TOFMS instruments. Thus most of the benefits of that technique apply here. The portion of ions analyzed by mass spectrometry is very high and arrival times correspond approximately with the CCS. Parallel fragmentation can be performed in a mode known as HDMS^E [141] where alignment of arrival times for peaks from parent ions and fragment ions can be used in very high throughput data-independent acquisition in proteomics experiments [27].

In addition to the many common attributes with nested IMS–TOFMS, TWIMS has a number of advantages due to the particular instrument arrangement, commercialization of the technique, and the maturity of the line of instruments. Ions in the most recent generation, the Synapt G2-Si, follow a trajectory from ion generation (typically ESI or MALDI) to a stepwave ion guide, a selecting quadrupole, a trap SRIG, a SRIG for ion mobility separation, a transfer SRIG, and finally a reflectron TOF mass analyzer. The stepwave ion guide is a novel method of purifying ions from uncharged solvent by directing primary gas flow along a linear path and using an effective electric field to direct ions into a parallel linear path and from there into the rest of the instrument. The selecting quadrupole can then be used to select ions by mass prior to ion mobility separation, or directed to pass all ions through. The trap SRIG is primarily to accumulate ions before injection into the ion mobility cell, but can also be used to hold ions for electron transfer dissociation or collision induced dissociation (CID) prior to mobility separation. Because injection from low pressure (such as the quadrupole) to higher pressure (where high pressure is desired for higher resolving power of ion mobility separation), the Synapt G2-Si uses two stages of drift gas to bring ions from low pressure to a higher pressure of helium (less massive and thus less ion losses upon injection) to the same pressure of nitrogen (more massive, but minimal losses upon injection from an equal pressure of helium) [105,165]. After ion mobility separation, fragmentation can be performed in the transfer SRIG in a manner analogous to parallel dissociation. Finally the reflectron TOF mass analyzer can be operated in “sensitivity” or “resolution” mode where ions pass through a reflectron either once for lower mass resolution but higher sensitivity or thrice for higher mass resolution but lower sensitivity.

The Synapt is a good example of inventive coupling to enable a range of operational modes from operation as a quadrupole-TOF mass spectrometer with the SRIGs evacuated of buffer gas, to a MS–ETD-IMS–CID-MS type instrument if selecting by mass in the quadrupole, fragmenting by ETD (or alternatively CID), separating by ion mobility, fragmenting again by CID, and then analyzing by TOFMS [167]. The ion mobility separation has two major parameters that can significantly impact operation, the velocity and height of the traveling wave. The combination of these two can be used to target select species with high resolving power in mobility terms, possibly even beyond that of a typical DT IMS of the same length, but also leads to a requirement of calibration against known standards, a restriction of the range of mobilities that are optimally resolving, and more heating of the ions. Because of the traveling wave nature of the ion mobility separation, determination of the CCS from the

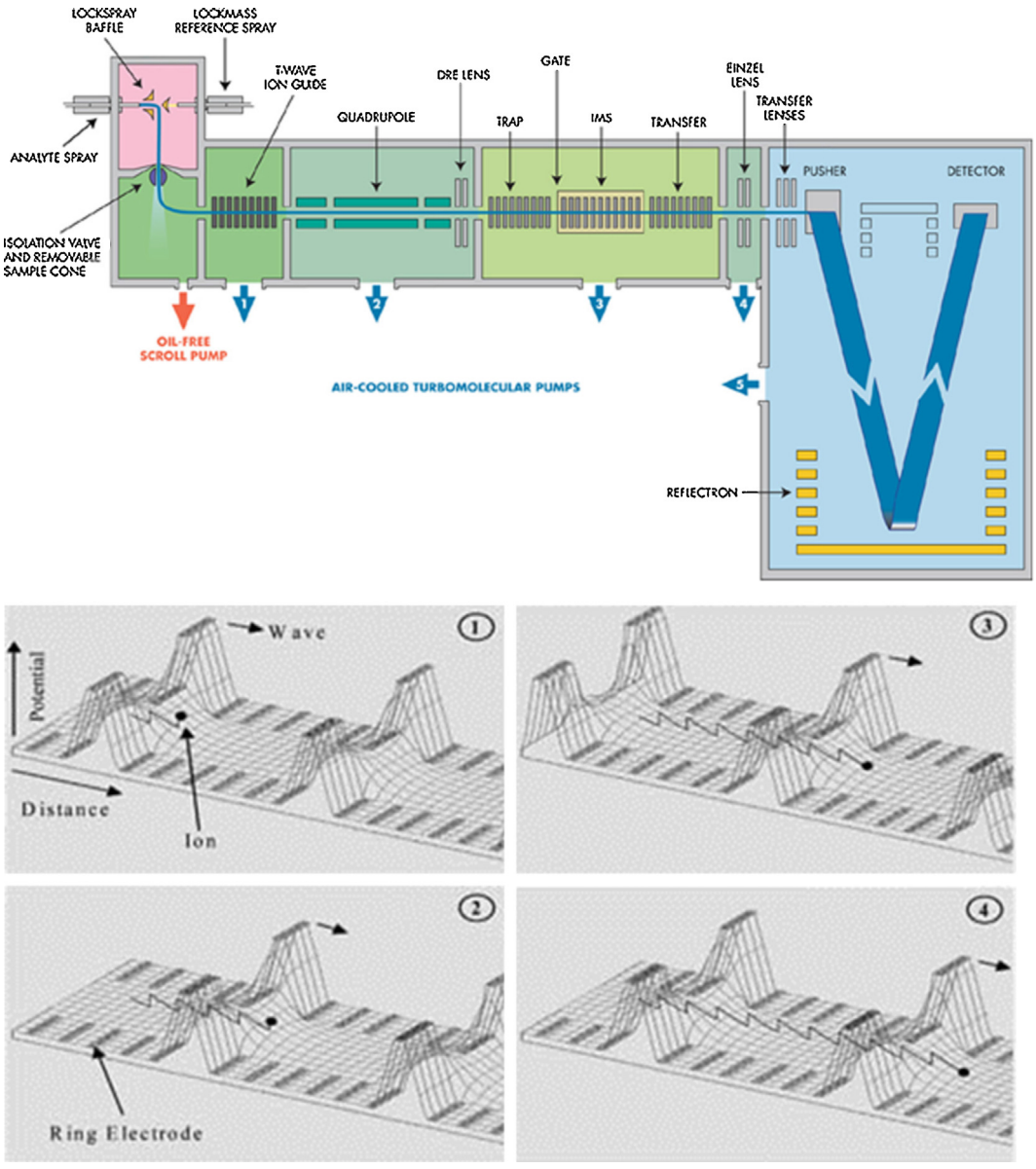

Fig. 6. Schematic of a Synapt G2 instrument showing ion generation through electrospray ionization, optics to guide ions through a quadrupole to the ion mobility cell and then on to the time-of-flight MS. Bottom: Method of propagation of ions of different mobilities in traveling wave ion mobility spectrometry where ions surf the wave as it propagates down the stacked ring ion guide from left to right. Smaller ions (of the same charge) typically have higher mobilities and travel farther under the influence of an electric field over a given period of time; larger ions lag behind. As the wave moves, fast ions surf the front of the wave for a higher percentage of time, always staying ahead of the wave ridge, while larger ions fall back over the wave, slowing down as they occupy a region with zero electric field before speeding back up as the next wave reaches them. At a constant velocity wave, ions reaching the exit of the stacked ring ion guide more quickly have been passed by fewer waves and thus the number of waves which pass an ion is directly proportional to the arrival time of the ion.

Adapted in part from the International Journal of Mass Spectrometry, 261, Steven D. Pringle, Kevin Giles, Jason L. Wildgoose, Jonathan P. Williams, Susan E. Slade, Konstantinos Thalassinos, Robert H. Bateman, Michael T. Bowers, James H. Scrivens, An investigation of the mobility separation of some peptide and protein ions using a new hybrid quadrupole/traveling wave IMS/oa-ToF instrument, 1–12, Copyright 2007, with permission from Elsevier [165]. Adapted in part from Ref. [66] with permission. Copyright© 2004 John Wiley & Sons, Ltd.

wave parameters is difficult [166], and in practice calibration standards are employed for which CCS values were obtained in linear DT IMS with nitrogen buffer gas. Waves that move too slowly and with too high of a peak height compared to the mobility of ions within the drift cell can cause ions to surf the wave, never rolling back over the traveling wave and thus taking the minimum time to transit the drift cell, the time for one wave to propagate from the beginning of the mobility SRIG to the end of it [165]. If multiple ions have high enough mobilities to surf the wave, there is no significant separation of these ions in the T-wave [165]. In practice the ability to tune both the velocity and height of the wave results in a range of mobilities separated efficiently by the T-wave that is broad enough that ions not separated are typically only those not of interest. Finally, there is some heating of ions in TWIMS [168], sometimes several hundred degrees worth of heating [169,170], sometimes very small amounts of heating [166]. The heating of ions is more significant for smaller ions and thus ion structure for peptides and small proteins can be quite different from that measured in the low-field regime of a linear DT IMS instrument [170].

Resolving powers for the Synapt-G2 instruments have been reported to be ~45 [105], high for a short 28 cm long SRIG with ~3 mbar of pressure. Additionally, a new circular TWIMS drift tube under development promises significantly higher resolving powers and is discussed below. Because of the maturity of Synapt line, the

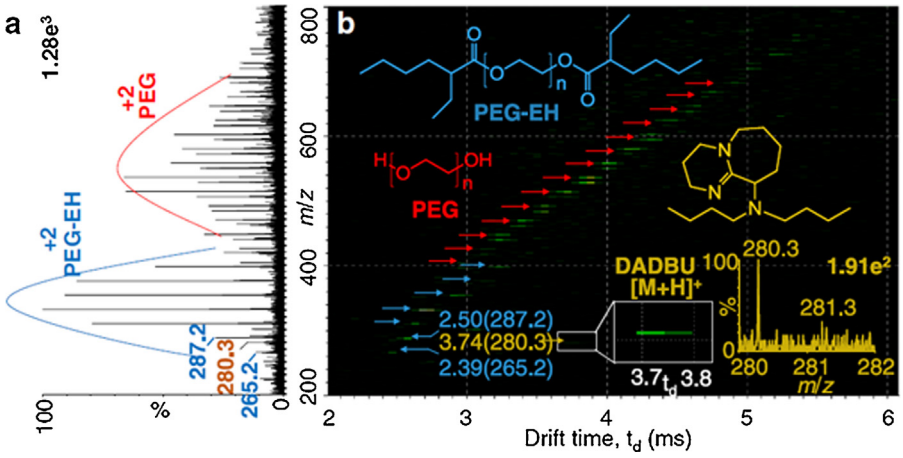

Fig. 7. TWIMS–MS spectrum of a model mixture of polymer PEG 1000, plasticizer PEG-EH 640, and property modifier DADBU generated using matrix assisted ionization vacuum on a Synapt G2. Total mass spectrum on the left and two-dimensional nested IMS–MS plot on the right.
Reproduced from Ref. [50] with permission from John Wiley and Sons.

software has been well-developed, and many experiments have been well-developed on this line of instrumentation. In particular the HDMS^E has been combined with liquid chromatography for impressive proteomic separations. Recently, almost 50,000 peptides were fragmented and identified from a single LC–IMS–MS run using an adjustable CID fragmentation energy in the transfer cell [27]. Numerous systems have been characterized by TWIMS–MS including polymers shown in Fig. 7 [50]. In a manner similar to that observed for nested IMS–MS, Fig. 7 demonstrates the power of TWIMS–MS in separating components of a mixture of species that overlap in the mass spectrum based upon their mobilities. As in IMS–MS, regions of the spectrum are extracted for analysis in either the m/z or drift dimensions as needed to fully explore the data.

2.1.3. Tandem ion mobility spectrometry–mass spectrometry

While the nested IMS–MS measurement is very efficient, the determination of an ion's mobility and mass is only a part of the story. Under many conditions, ions will undergo structural transitions in the gas-phase and the new structures that are formed often have mobilities that differ from the initial structures. This leads to additional separation strategies that have been termed IMS–IMS–MS [142]. In an instrument having a nested IMS–MS configuration, IMS–IMS techniques are employed in an instrument that utilizes multiple drift regions (for IMS–IMS two drift regions are used [142]; higher order separations, e.g., IMS–IMS–IMS or IMS^n can be carried out with three or more drift regions [171]). A schematic diagram of a simple IMS–IMS instrument is shown in Fig. 8 [142,172]. In this instrument a distribution of mobility separated ions is created in the first drift region. An ion selection gate can be used to select species with specific mobilities for ion activation. The activation process involves utilization of a higher field region to create energizing collisions and at elevated temperatures a new distribution of ion structures is generated. These are then separated in a second drift region in the typical nested IMS–MS fashion.

Collisional activation after one stage of separation and before another is very useful for structural applications such as identifying gas-phase energy barriers [164,173] and even using these barriers to determine how much of an effect solvent has on various structures [118]. Without collisional activation, IMS–IMS is identical to single stage IMS with a longer drift tube in DTIMS, or has a comparable increase in separation capacity for other techniques, with the notable exception of TM-IMS noted below where a second stage eliminates background signal from non-selected ions [174]. This can be used to advantage in the experiment, with only a change in potential needed to elicit a rapid conversion of an instrument from high resolution without activation to tandem IMS with activation and back.

With the advent of combing, tandem ion mobility separations show great promise for highly complex samples [172]. In combing, ions from the first stage of mobility separation are gated into the second stage in short windows interspersed such that the activation between the first and second stage of separation leads to almost complete coverage of the mobility spectrum in the second dimension but no more as conceptually demonstrated in Fig. 9. Ions that are selected in the same tooth of the combing experiment have approximately the same mobility before activation, but often activation will result in different enough mobilities to achieve separation in the second phase of separation. If ions were not pre-selected, then these activated ions would overlap with other ions, but by selecting and then activating, peak capacity can be dramatically increased [172]. With the rapid speed of gas-phase separations and high rate at which electrical potentials can be switched, combing can enable very high throughput and high peak capacity separations. There is a small cost in signal, a factor of 5 or 10 depending on experimental conditions chosen, but a dramatic increase in peak capacity, potentially greater than a 100-fold increase [172]. We expect that further developments in coupling of ion mobility techniques may significantly increase the peak capacity and thus separation capability of ions.

2.1.4. Trapped ion mobility spectrometry–mass spectrometry

TIMS offers a unique method of nesting ion mobility spectrometry with potentially any mass analyzer. Instead of a nearly stationary buffer gas as in DTIMS or TWIMS, trapped ion mobility spectrometry uses a high flow of buffer gas to push ions forward and a slowly adjusting electric field to restrain ions from entering the mass analyzer as shown in Fig. 10 [69,175,176]. The retarding electric field is ramped from a high electric field that retards all ions to a low electric field to retard effectively no ions, allowing the flowing buffer gas to carry ions of interest into the mass spectrometer for mass analysis. Because the electric field acts to retard ion motion instead of directing their motion, TIMS ejects ions with larger CCS before ions of smaller CCS, giving an inverted drift spectrum relative to DTIMS and TWIMS [69]. Like many other axial dispersion ion mobility separations, TIMS uses rf confinement to minimize loss of ions to collisions with the lenses and walls of the device [69]. One major advantage of TIMS instruments is their small size, typically only 5–10 cm long, and the independence of length and resolving

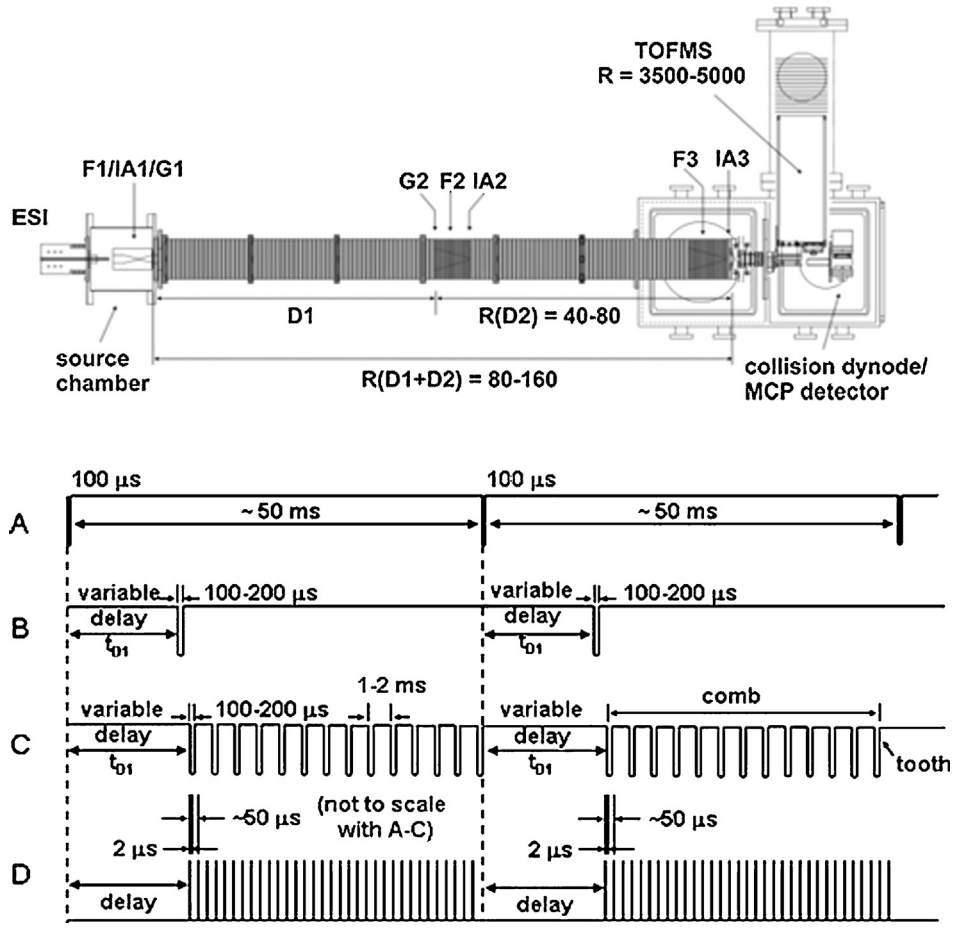

Fig. 8. Top: Schematic of an IMS–IMS–MS instrument. Bottom: accompanying pulse sequence for which gates are pulsed. Ions are generated by ESI on the left, accumulated in a Smith-geometry ion funnel before being pulsed into drift region D1 at the pulses shown in (A). Selection of ions by mobility is achieved at gate G2 (B) in a singular fashion or in a combing fashion (C). Finally, the TOF is pulsed continuously (D) in order to obtain m/z for all ions as they exit drift region D2 and enter the TOF.

Adapted in part with permission from S.L. Koeniger, S.I. Merenbloom, S.J. Valentine, M.F. Jarrold, H.R. Udseth, R.D. Smith, D.E. Clemmer, An IMS–IMS analog of MS–MS, Anal. Chem., 78 (2006) 4161–4174. Copyright 2006 American Chemical Society [142]. Adapted in part with permission from S.I. Merenbloom, S.L. Koeniger, B.C. Bohrer, S.J. Valentine, D.E. Clemmer, Improving the efficiency of IMS–IMS by a combing technique, Anal. Chem., 80 (2008) 1918–1927. Copyright 2008 American Chemical Society [172].

power. In DTIMS and TWIMS, increased drift tube length leads to increased resolving power, and lab footprint can often be a practical consideration in limiting instrument resolving power when other constraints are included, but this is not as significant of a concern with TIMS [176,177].

Engineering the fine control of gas with minimal turbulence is more difficult than the fine control of electric field which is why a single buffer gas flow rate is used to direct ions toward the mass spectrometer with a variable electric field to select ions by mobility [178]. The resolving power is controlled by the velocity of the buffer gas, the electric field ramp speed, and the rf confinement. Increasing the velocity of the buffer gas increases the required retarding electric field for ions to be trapped which can lead to the high-field limit or electrical breakdown at the extremes, but not before resolving powers consistently of 250 can be achieved [138,177–179]. Slower ramping of the electric field leads to slower rates of ejection from the TIMS device into the mass analyzer, requiring longer trapping before the TIMS device, hindering limits of detection as the efficiency of ion trapping at higher pressures drops dramatically as the time of ion trapping increases [148,180] and TIMS can have the longest ion trap times of any technique described herein [178]. Current research, as for all ion mobility techniques with accumulation prior to analysis, involves increased efficiency of pre-mobility trapping; significant strides toward this has recently been accomplished for rapid analyses [181]. Long trap times may also be problematic for structural analyses as some structures [132,133] have been shown to change over time in the gas-phase. The ability to change the trap time could however open up experiments examining the evolution of structure over time in the gas-phase in experiments complementary to those performed previously [132]. A final concern with TIMS for structural analysis is the applicability of the fields. The equations derived for structural analysis all depend on the relative motion of the ions and the buffer gas and the comparison to the uniformity of the fields, but the changes in fields in different regions of the instrument could lead to differences in structural determination between this technique and more traditional drift tube analyses. Despite these differences, TIMS–MS analysis of ubiquitin structure shows results that compare favorably with measurements from DTIMS as shown in Fig. 11 [182]. A number of voltages clearly influence the temperature of the ions and thus the distributions of conformers, with compact, partially folded states, and elongated states observed in different ratios depending upon the specific applied voltages, a consistent theme amongst IMS–MS experiments where particular care must be taken in understanding the instrument voltages on the cross-sections measured. We look forward to seeing more studies comparing protein structures between them in order to ascertain the magnitude of this effect.

The ability to change the ramp rate and even to make the ramping discrete [183] makes the technique particularly suited for

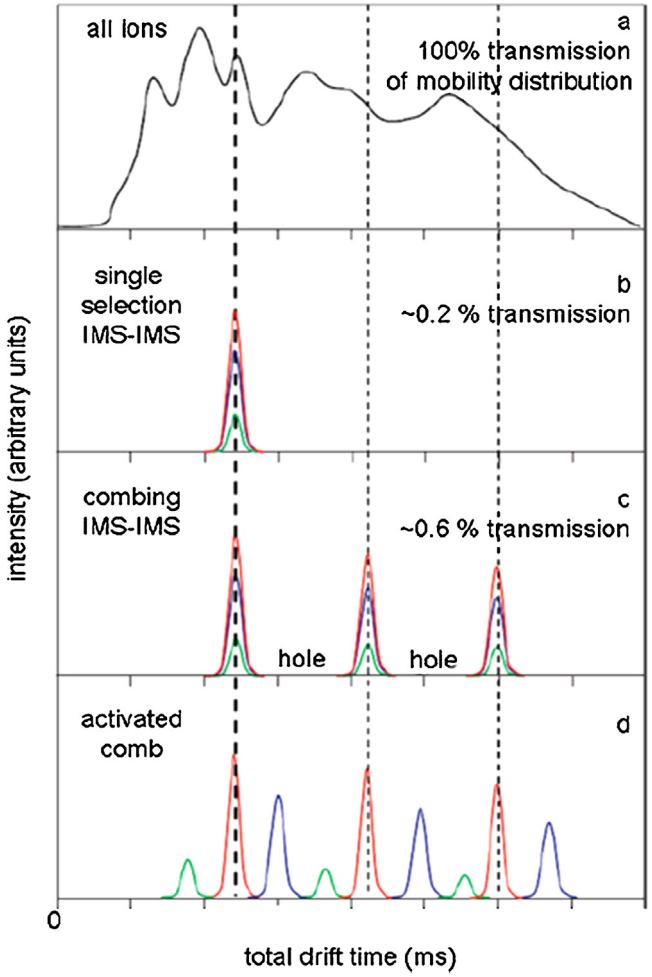

Fig. 9. Method of combing in IMS–IMS. (a) Hypothetical summed distribution of all mobilities from a complex mixture. (b) Single selection from the hypothetical distribution with different colors under the primary peak indicating multiple overlapping species that will separate after activation. (c) Combing-selection of multiple teeth from under the entire distribution, each with several species under a single peak. (d) Activation after combing showing that species with the same mobility in the first dimension of IMS change differently upon activation and separate, filling up the spectrum while reducing overlap between different species. (For interpretation of the references to color in this figure legend, the reader is referred to the web version of this article.)

Reprinted with permission from S.I. Merenbloom, S.L. Koeniger, B.C. Bohrer, S.J. Valentine, D.E. Clemmer, Improving the efficiency of IMS–IMS by a combing technique, Anal. Chem., 80 (2008) 1918–1927. Copyright 2008 American Chemical Society [172].

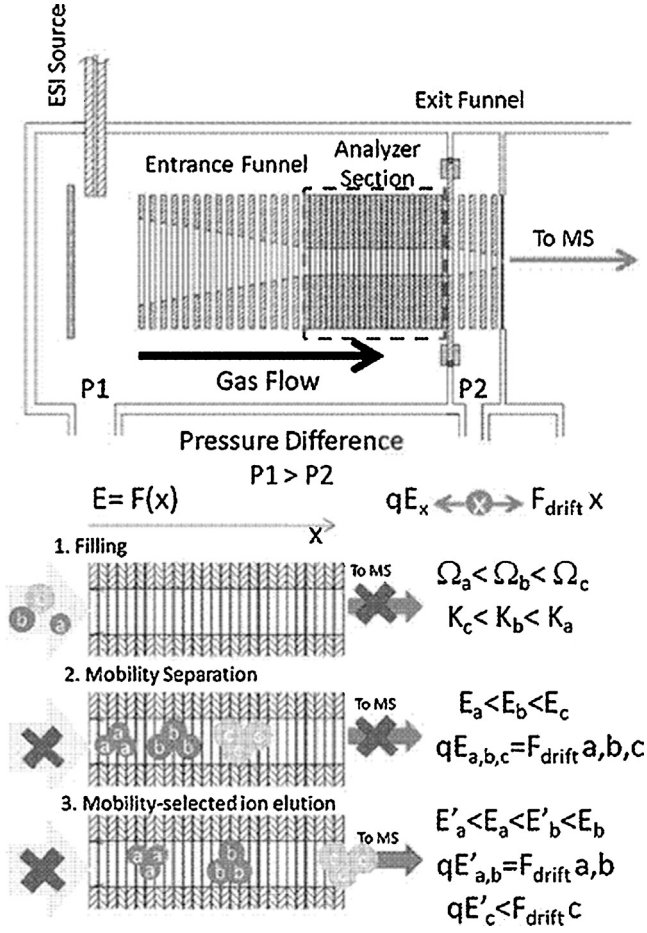

Fig. 10. Schematic and method of elution of ions of different mobilities in trapped ion mobility spectrometry. Ions enter from the left pushed by the flow of gas and are trapped in an ion funnel trap by the high electric field retarding from the right. As the retarding potential is reduced, the field, and thus the force, $F = q \cdot E$ (where q is the charge), on the ions buffer-gas directed pressure-dependent force to determine net movement, reduces and ions propagate into the mass analyzer.

Reprinted with permission from Ref. [69] with kind permission from Springer Science and Business Media.

dispersive analysis with slower mass analyzers such as FTICR–MS and IT–MS, although longer separation times must also be reconciled with liquid-phase separations prior to TIMS–MS for broadest applicability. Unfortunately, this technique is still in early development and has yet to be commercialized but shows great potential as an alternative dispersive ion mobility separation and in coupling a dispersive ion mobility separation with mass analyzers other than an orthogonal TOFMS, including an FTICR–MS [183].

2.2. Selective ion mobility spectrometry techniques coupled to mass spectrometry

In addition to nested ion mobility techniques, there are many methods for transmitting ions of only a selected mobility and then analyzing the resultant mass spectrum or vice versa. In these techniques, a two-dimensional spectrum is obtained by scanning the selection method and stitching together a spectrum from the sum of multiple mass spectra across different transmitting mobilities or from the sum of multiple drift spectra across different mass-to-charge ratios. Ions that are not selected are lost, neutralized on lenses that are at the minimum potential reached from the ion trajectory [83] or within the selective mass spectrometer. The ideal mobility-selective technique would neutralize no ions of the desired mobility with the ability to completely and instantly tune the width of transmitted mobilities. Thus the selective technique could be used to pass ions of all mobilities or of only the desired mobility as befits the experiment. Selective techniques will often do better in cases where dispersive instruments are not as well-suited such as slower mass analyzers like ion trap mass spectrometers [26,184–186], Fourier transform ion cyclotron resonance (FTICR) [187,188] and Orbitrap mass spectrometers [189]. Uses include increasing signal to noise by reducing chemical noise [190], purification of a desired charge state [185], the latter also for less common post-mobility separation analyses such as cold ion traps [191] and laser-induced fluorescence [188].

Among the most powerful uses is the ability to perform MS^n ($n > 2$) after mobility selection. While parallel fragmentation enables MS^2 after dispersive ion mobility separations, coupling to e.g. an ion trap mass spectrometer via selective ion mobility separations can lead to the harnessing of the immense and well-developed power of repeated fragmentation steps. Despite

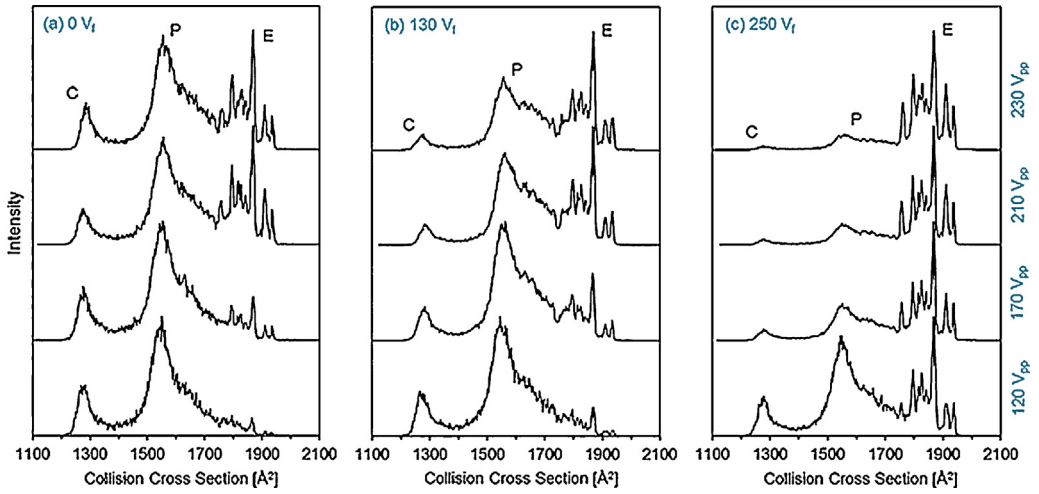

Fig. 11. Distributions of ubiquitin $[M+7H]^{7+}$ across different DC voltages applied across the entrance funnel (V_f) and peak-to-peak RF voltage amplitudes (V_{pp}). Distributions show significant resemblance to previous work [116,117] and demonstrate the effect of increasing voltage on heating of the ions as compact portions of the distribution decrease with increasing V_f and V_{pp}.
Adapted from Ref. [182] with permission of The Royal Society of Chemistry.

coupling of ion mobility to ion trap mass spectrometers with CID [26,185], VUV-PD [186], and ETD [26], most experiments, with the notable exception of FAIMS [184,185,192], have been on prototype instruments with proof-of-principle experiments and only a few have seen regular use. The utility of coupling FAIMS to ion traps for MS^n [184,185,192] has demonstrated the combination of selective mobility separations and MS^n for $n > 2$ is an underdeveloped area in tandem IMS–MS experiments.

In this section we discuss selective DTIMS, DMA, FAIMS and DMS (here grouped with FAIMS), OMS, circular ion mobility techniques, and TM-IMS as mobility analyzers to couple to mass spectrometers. Of these techniques, FAIMS stands out as unique in that it separates by the ratio of mobilities at high and low fields rather than directly on the mobility at a given electric field, as described in more detail below. As trapping technology improves, there remains the question of whether a selective technique could recycle ions back to the entrance region, or trap them for later analysis when the scan of the mobility selection reaches the appropriate value. This recycling of ions for repeated analysis mirrors some portions of circular techniques and could overcome one of the largest potential limitations of these techniques, the high limit of detection when obtaining a complete mobility spectrum of a single sample.

2.2.1. Selective drift tube ion mobility spectrometry coupled to mass spectrometry

The traditional ion mobility separation device was the linear drift tube ion mobility spectrometer. Ions are produced by a source, often accumulated, and then enter the drift tube through some entrance gate. The entrance gate synchronizes ions as they enter the drift tube in order to ensure accurate measurement as they exit the drift tube. A spectrum of ion intensity compared to the time to transit the drift tube is often called a mobility distribution although there are many names found in the literature including drift distribution, arrival distribution, and mobilogram. While continuous measurements of signal or current over drift time are common in stand-alone linear drift tubes, a full mobility spectrum could not be collected at the same time as a full mass spectrum in the original instruments. As described above, the earliest drift tubes were all employed in a selective fashion, either selecting by mass or by mobility.

Because this method of coupling makes no requirements about the relative analysis times of the coupled techniques, it is of particular interest when coupling to quadrupoles [162,193–195], sector mass spectrometers [196], ion traps [186], and even cold ion traps [191]. Because of the maturity of a linear drift tube, the simplicity of construction, and large number of experimentalists experienced with drift tubes, this can be quite beneficial when a high fidelity mobility filter is desired. Resolving power will match that of nested DTIMS–TOFMS, but a full spectrum typically requires a scan and thus sensitivity can only be matched for a single ion, not for the entirety of a complex mixture. If only one ion is of interest, such as in cold ion traps, this is a reasonable technique of choice, but it fails to take advantage of the natural nesting between DTIMS and TOFMS and requires trapping before analysis similar to all dispersive techniques and separate from many other selective techniques. While trapping can often be done efficiently, it is difficult to eliminate ion losses when trapping, especially at longer time periods and current research often focuses on improving ion accumulation and transmission [148,180,197].

To increase signal, entrance and exit gates can be pulsed in a matched fashion to allow overlap of signals at a given exit gate pulse with mobility deconvolution using Fourier [198–200] or Hadamard [140,201–203] techniques. The resulting increase in sensitivity improves resolving powers and enhances the use of selective DTIMS for high resolution mass spectrometry. Several companies now sell versions of this separation including TOFWERK for an all-encompassing IMS–TOFMS system [140] and Spectroglyph for attachment to an Orbitrap [204].

2.2.2. Differential mobility analysis–mass spectrometry

DMA takes the idea of directing ions by their electric field against a retarding buffer gas and flips it on its head, having the buffer gas push the ions orthogonal to the electric field and determining whether the ions can pass from one slit to another as the electric field is varied, as shown in Fig. 12. Like most of the selective techniques discussed here, DMA transmits ions of a given mobility and a scan of the electric field is required to obtain a full spectrum of ions by mobility. DMA has its roots in aerosol analysis [70] and was modified to enable molecular analysis [70,73,74] and then coupled to mass spectrometers [205] where it has seen extensive use in examining structural transitions of families of ions of clusters and polymers, the latter shown in Fig. 13. DMA allows a continuous stream of ions, an improvement over the use of DTIMS as a selective technique where ions must be trapped and injected into the drift tube and losses can be expected in the process of trapping ions. While ion funnels have reduced pre-mobility separation

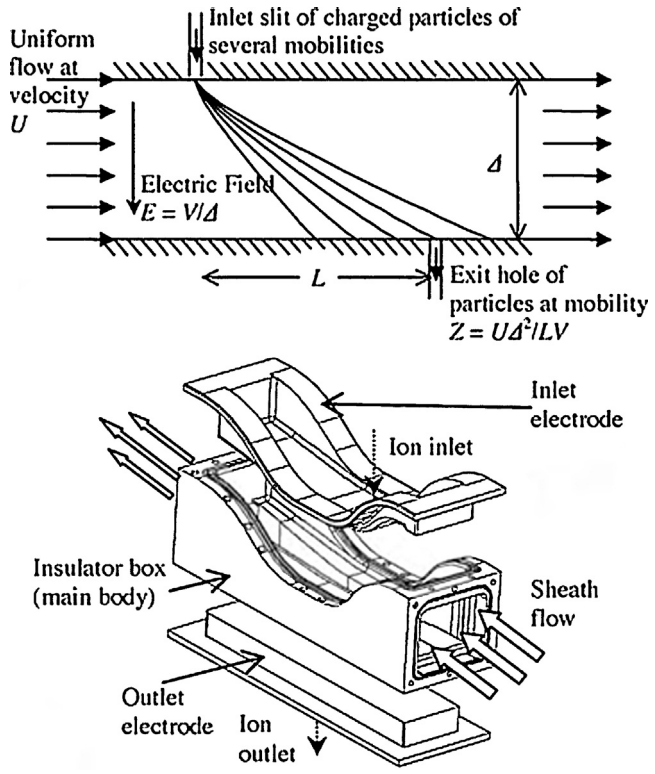

Fig. 12. Top: Method of separation of ions by differential mobility analyzer. Ions are injected along an electric field going from top to bottom. An orthogonal flow of gas from left to right pushes ions down from the inlet slit toward the exit slit. Ions whose mobility match the length from inlet slit to exit slit, the flux of the flowing gas, and the electric field as given by the equation in the figure (where Z is mobility and L is the width of the slit) will reach the exit slit and leave the tube. Ions whose mobility does not match these parameters will not exit the tube and will instead be eliminated on the lens that acts as the wall. Bottom: Schematic of physical DMA cell.

Reprinted from the International Journal of Mass Spectrometry, 298, Juan Rus, David Moro, Juan Antonio Sillero, Javier Royuela, Alejandro Casado, Francisco Estevez-Molinero, Juan Fernández de la Mora, IMS–MS studies based on coupling a differential mobility analyzer (DMA) to commercial API–MS systems, 30–40. Copyright 2015, with permission from Elsevier [72].

losses down to low levels in DTIMS, there are still small losses if the outlet stream is discontinuous due to the use of a gate as in selective DTIMS. DMA devices in contrast have losses due to a lack of focusing (e.g. rf focusing as in TWIMS, DTIMS, and TMIMS) and diffusion of ions beyond the width of the exit slit, the latter can be adjusted by changing the width of the slit where increasing width reduces resolution but increases signal [70].

Additionally, DMA devices are often operated at atmospheric pressure whereas most modern DTIMS and TWIMS instruments operate at reduced pressures [98]. As a result, any concerns about changes in the structure of ions upon going from higher to lower pressure regimes are mitigated until after mobility separation, a benefit or a disadvantage depending upon the experiment [98]. Because DMA–MS can be run with a low electric field, most ions can be examined in the low-field regime, although ions with high enough mobilities may require high electric fields to counter the flow of gas. Since the low-field regime is defined by E/p, the higher pressure of a DMA instrument means that in practice almost all experiments are done in the low-field regime, DMA–MS is particularly useful as a selective filter in the low-field regime.

The limiting factor on the resolving power of most current DMA instruments is the control of the flow of buffer gas relative to the inlet and outlet slits. Small manufacturing defects can result in turbidity at high gas-flows and large instruments, resulting in dispersal of a species of ions of the same mobility relative to the average path of that species and as a result DMA resolving powers are typically a bit lower than top-end DTIMS instruments although commercial DMA–MS, DTIMS–MS and TWIMS–MS instruments offer comparable resolving power in the mobility dimension. With offset slits and the high flow of gas, no current DMA can easily by set to transmit ions of all mobilities, a highly desirable feature in an ideal selective technique. As the oldest, most well-understood, and robust continuous ion mobility filter for low-field experiments, DMA instruments for coupling with mass spectrometers have many advantages and have been commercialized by SEADM (Boecillo, Spain). Although most DMA instruments have been coupled to quadrupole and quadrupole-TOF mass spectrometers [72,206,207], they have also been extended to FTICR mass spectrometers [188] and we expect other variations to surface in the near future as their low-field and structural selectivity makes for a good fit with more detailed post-mobility-selection analyses and their recent availability by SEADM makes for ease of coupling to mass spectrometry.

2.2.3. Field asymmetric waveform ion mobility spectrometry–mass spectrometry and differential mobility spectrometry–mass spectrometry

FAIMS is known by a number of names including DMS and Differential Ion Mobility Spectrometry (DIMS). In this review we will use the abbreviation FAIMS to avoid confusion with DMA, although FAIMS and DMS often refer to slightly different geometries [208,209]. FAIMS was originally developed in the USSR [208] before significant development was done in coupling to mass spectrometry by Guevremont and coworkers [17,76,190,210–214]. Shvartsburg and others have since drastically increased the resolution of FAIMS and DMS devices [22,137,208,215,216]. For a more detailed history of FAIMS and DMS and some recent developments in applications and buffer additives to improve resolution, we refer the reader to a recent review by Schneider et al. [208].

Unlike all other techniques discussed in this review, FAIMS does not separate directly on the basis of mobility, but rather by the ratio of low-field to high-field mobilities, and thus the separation is orthogonal to the m/z measured by a coupled mass spectrometer. The orthogonality of the separation leads to high peak capacities for FAIMS–MS and as a result this technique has become very popular. Because of the overlap in physical parameters – ion mobility being core to both separation techniques – FAIMS is often linked to ion mobility spectrometry. We discuss FAIMS in brief in this review as it is a gas-phase technique with very similar characteristics to the many other selective ion mobility separation techniques, and because the separation principle has significant overlap.

The two main geometries are a cylindrical geometry known as FAIMS and a geometry using two flat plates known as DMS [208]. For simplicity we will refer to the flat geometry when discussing ion motion despite our use of the term FAIMS as the separation principle is the same, only the geometry and attendant device characteristics differ. As shown in Fig. 14, ions enter from an entrance slit and traverse between two plates toward an exit slit. The field between the two plates is alternated, in one phase a relatively low electric field is typically applied for longer periods of time and directing ions toward one plate while a high electric field is typically applied for shorter periods of time and directing ions toward the other plate. A DC offset is applied to the entire set of applied electric fields such that the time-average of the low and high electric fields is not zero, and this offset, known as the compensation voltage (CV), is scanned. Ions whose mobility in the low and high electric fields will traverse the two plates and exit device at CV = 0 V, whereas those whose mobility is greater in the high electric field phase will need an opposite sign of the CV to traverse the device compared to those whose mobility is greater in the low electric

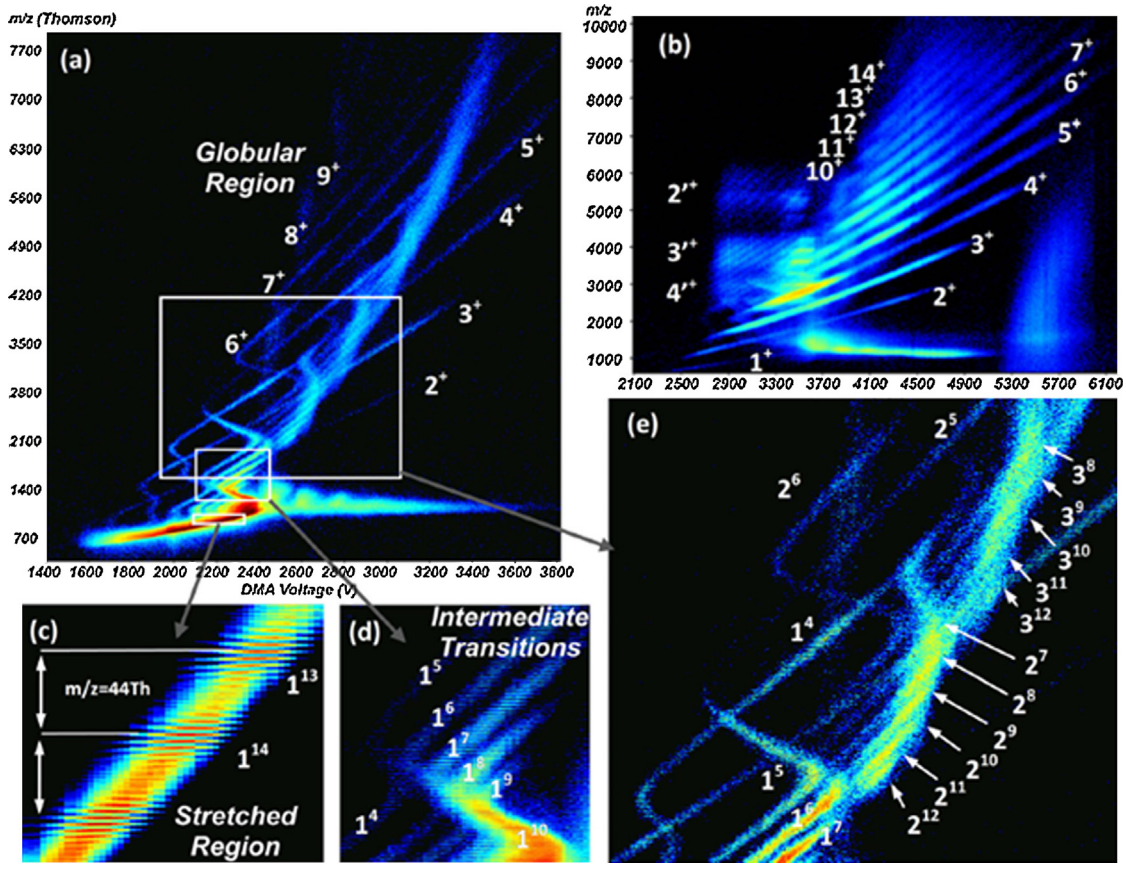

Fig. 13. DMA–MS spectra for polyethylene glycol generated by electrospray ionization. Structural changes can be seen within families of similar ions as the m/z increases. (a) shows the full two-dimensional spectrum whereas the remaining panels show expanded portions of the spectrum. The notation x^z denotes the level of aggregation (x) and the charge state (z).

Reprinted with permission from Ref. [51] with kind permission from Springer Science and Business Media.

field phase. A full spectrum is collected by scanning the CV, and therefore FAIMS, like DMA, is a selective scanning technique.

FAIMS has become a very popular technique as a result of its orthogonality to mass spectrometry, where the CV is not tied to the m/z as is the CCS and mobility determined in DTIMS, TWIMS, DMA, or any other technique discussed herein. However, this same

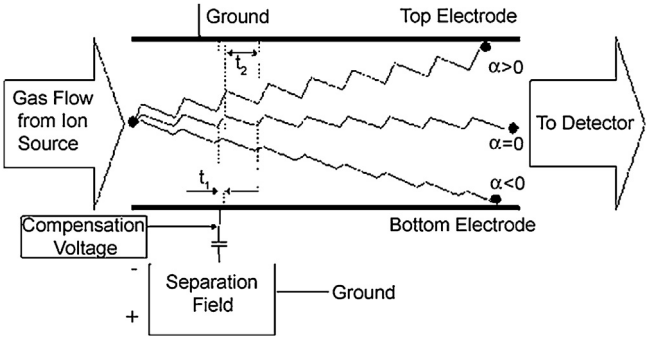

Fig. 14. Method of separation of ions in FAIMS/DMS. The shorter time period but higher electric field is applied going up while the longer time period but lower electric field is applied down in the example shown here, with compensation voltage applied. $\alpha > 0$ denotes an ion that moves farther during the higher electric field than the lower electric field and do not reach the exit slit before being neutralized on the lens that acts as the wall, in contrast to $\alpha < 0$ which denotes the opposite net motion (farther in the lower electric field) but also does not exit the device. $\alpha = 0$ denotes ions that move equally in both directions and exit the device at the given compensation voltage.

Reproduced from Ref. [209] with permission of The Royal Society of Chemistry.

orthogonality makes determination of the CCS in the same manner as IMS impossible [17]. As a selection technique, FAIMS or DMS is among the most mature, with several companies making commercial FAIMS instruments for coupling to mass spectrometers, including Ionalytics owned by ThermoFisher, Sionex in collaboration with AB Sciex to make SelexION, Owlstone, and GAA Custom Engineering. Extremely high resolving powers of several hundred have been achieved [137,216]; however, the resolving power of FAIMS does not directly compare to the resolving power of any other technique within this review, as the separation phenomenon is different, the scaling of the axes are quite different, and in some cases each technique will be preferable. Shvartsburg et al. have discussed the possibility of higher order techniques that use more complex waveforms and higher electric fields beyond those found in FAIMS [217]. The alignment of the entrance and exit slit for FAIMS devices means that this technique can be set to have no oscillating waveform in order to pass through all ions regardless of mobility, although the small size of the devices used to achieve the highest resolving powers may lead to diffusion of the ions and loss against the walls of the device if pressure is not reduced. Since pressure cannot be instantly tuned, the ability to rapidly switch between selective transmission and broadband transmission without loss of signal can be hindered in some geometries and experimental conditions.

Improvements in instrumentation have led to the change from a cylindrical geometry where ions are traversing from slit to slit between two cylindrical electrodes, to a planar geometry where ions travel between two planar electrodes [208,209]. This geometry in concordance with constant improvements on electronics, machining tolerances, changes in buffer gas, and the ability to

make smaller devices has led to improvements in transmission efficiency and resolving power. Such devices have been coupled to quadrupoles [76], TOFMS [210], quadrupole-TOFMS [214], ion traps [184,185,189,192,218], FTICR-MS [187,219], orbitraps [185,189], and cold ion traps [191]. A wide variety of applications have seen the use of FAIMS, among them attempts to solve how much structural information can be gleaned from FAIMS–MS, where different charge states of cytochrome *c* are shown in Fig. 15, which despite the natural heating of FAIMS still shows multiple peaks that appear to be distinct conformations [137]. The new high resolution FAIMS instruments are helping to separate out these different states.

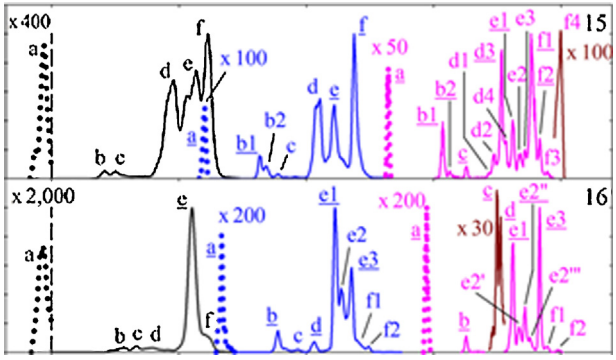

Fig. 15. FAIMS spectra of $[M+15H]^{15+}$ and $([M+16H]^{16+}$ charge states of cytochrome *c* in different gas conditions from pure N_2 (black/left, magnified portions as dashed lines) to 50% N_2/50% H_2 (blue/center, magnified portions as dashed lines), to 16% N_2/84% H_2 (pink/right, magnified features in maroon). Increasing amounts of H_2 enabled higher resolution and thus elucidation of more conformers across the different charge states.

Reprinted with permission from A.A. Shvartsburg, Ultrahigh-resolution differential ion mobility separations of conformers for proteins above 10 kDa: onset of dipole alignment?, Anal. Chem., 86 (2014) 10608–10615. Copyright 2014 American Chemical Society [137].

2.2.4. Overtone mobility spectrometry–mass spectrometry

OMS uses a segmented drift tube with alternating electric fields along the axis of ion propagation to select ions of a given mobility with the frequency of field alternation determining the mobility of transmission [78]. The segmented drift tube is made up of alternating elimination and transmission regions [78]. The electric field in transmission regions is constant and only the applied voltages changes to generate a sawtooth waveform where the electric field in elimination regions alternates between forward and backward as shown in Fig. 16. A significant fraction of ions whose mobility matches the frequency of field application will traverse the drift tube coincident with the transmitting (forward propagating) field

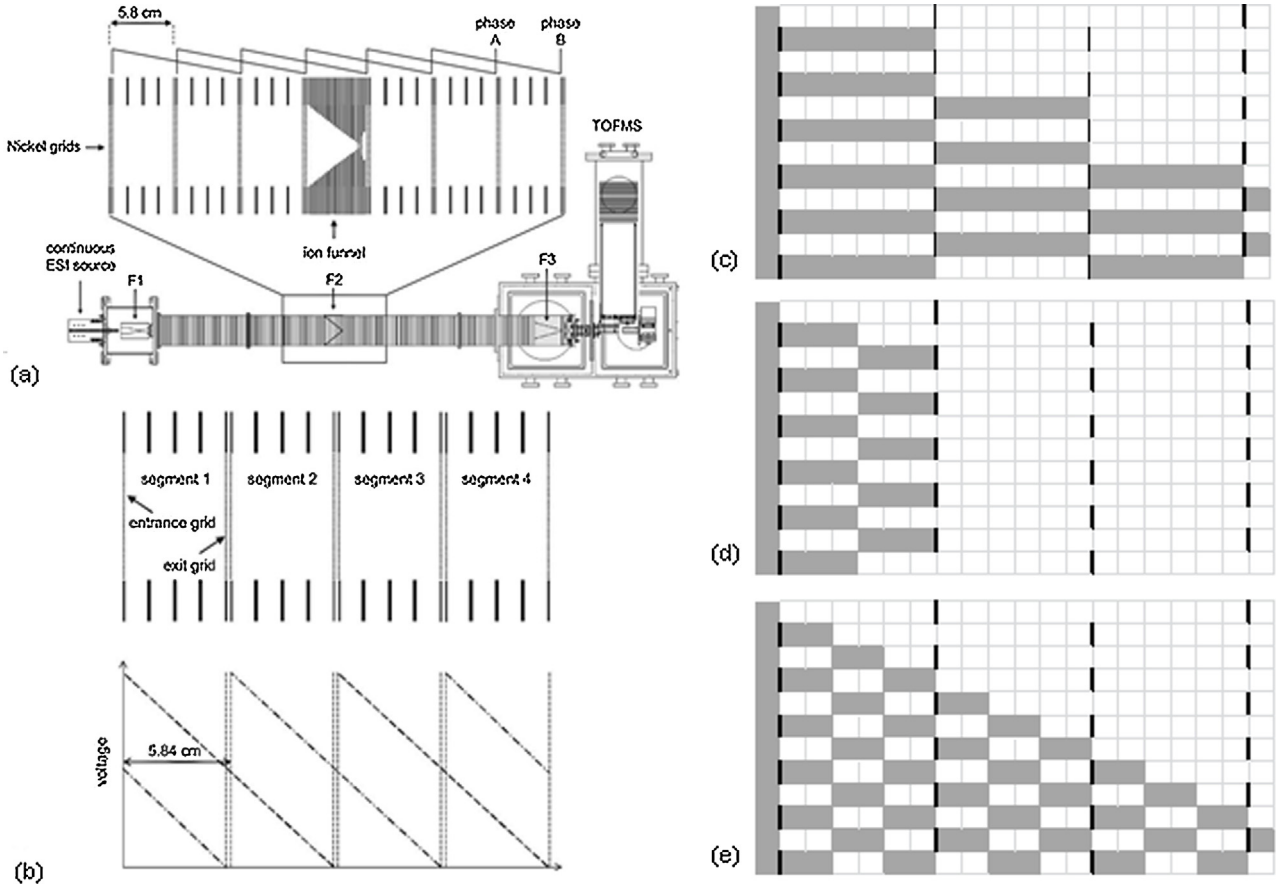

Fig. 16. (a) Instrument schematic for OMS showing segmented drift tube with a funnel midway through the drift tube for radial focusing. (b) Applied potentials for the method of separation of ions in OMS for the simplest case, two-phase OMS where two phases are shown, denoted as phases A and B above the expanded portion of the drift tube. (c–e) Phases are alternated for equal periods of time, each period of time shown as a line, visualized as a snapshot at the beginning of that period of time of where ions fill the instrument. Elimination regions are lines containing darkened bars, where the darkened bars are elimination regions that are active – that is ions that traverse into them are eliminated. Undarkened bars are for ease of viewing only. (c) Ions at the fundamental frequency traverse one segment per phase and the entire drift tube as shown in the bottom left. (e) When the fields are applied three times as fast, ions traverse 1/3 of a segment per phase and also traverse the entire drift tube as shown in the bottom right. (d) At a frequency of twice the fundamental frequency, as shown in the top right, ions only traverse half a segment each phase and are eliminated quickly, never reaching the end of the device.

Adapted with permission from Ref. [78] with kind permission from Springer Science and Business Media.

in the elimination regions, whereas all ions whose mobility does not match the frequency of field application will reach an elimination region when the field is eliminating (propagating toward the nearest lens or grid rather than toward the detector) and the ion will be directed toward lenses upon which it will neutralize [77,78,220,221]. As such OMS selects ions by mobility based upon their axial motion in a varying electric field analogous to cars attempting to make it through a series of red lights at constant velocity.

The resolving power of OMS scales well with length, nearly linearly in some cases, dependent upon a number of variables [77,78]. Because of the mode of operation of the elimination regions as a series of gates, diffusion has less of an effect in reducing resolving power than is seen in DTIMS. A more complete treatment of resolving power can be found in Ref. [143] but it should be noted that only estimates for upper and lower bounds for resolving power can be derived analytically, a complete determination of resolving power requires numerical integration from the convolution of Gaussians with boxcar functions. Because of the favorable scaling with length, the theoretical miniaturization of OMS compares favorably with IMS, and resolving powers for 2 meter instruments have exceeded 200 [133]. OMS is typically operated in the low-field regime, similar to DTIMS, and the difficulties increasing resolving power by increasing the electric field are exacerbated by the increased voltage, and thus increased likelihood of electrical breakdown, across eliminating elimination regions. The near-continuous beam exiting an OMS device makes OMS a good technique for coupling to techniques where the isolation of a single mobility or structure is desired as the requirements on trapping at the front of the drift tube are less. Because OMS resolving power increases with increasing overtone, the technique can often be set to transmit a wide range of mobilities at low overtones and a narrower range with increasing overtone with the only difference between the frequency at which the potential waveform is applied. This rapid switch is mitigated by the incompleteness of the switch, where the low overtones do not pass all mobilities but instead a broad range, and the high overtones suffer from loss of signal [221].

Original instrumentation demonstrated the proof of concept of OMS but newer instrumentation has removed the grids used to define the electric fields, instead using a radial eliminating field to move ions to the lenses and an axial propagating field with rf confinement to transmit matched mobilities [104]. This gridless OMS device had limits of detection in the low attomole range when coupled to a home-built TOFMS and inserted into a longer linear DTIMS device [104]. Overtones of the fundamental peak occur in OMS where they are useful in improving resolving power [77,78,133] and as shown in Fig. 17 but can also result in overlapping overtones that make identifying peaks difficult. A new method of selecting the transmitting overtone or overtones (selected overtone mobility spectrometry – SOMS) by changing the ratio of lengths of time that different phases are pulsed has recently expanded the overall peak capacity of the OMS technique [222]. At present all OMS instruments have been couple to TOFMS instruments, but we expect that OMS will find use in low-field isolation of gas-phase ions by structure prior to more involved analyses.

2.2.5. Circular ion mobility spectrometers coupled to mass spectrometers

While the resolving power of a DTIMS instrument is proportional to the square root of the applied electric field, the electric field itself is often limited to achieve separation in the low-field regime for reasons described above. At a given applied electric field, among the easiest methods of increasing resolving power for a given class of species is increasing the length; however, the resolving power scales with the square root of the length, and thus diminishing returns and practical constraints on instrument length often limit

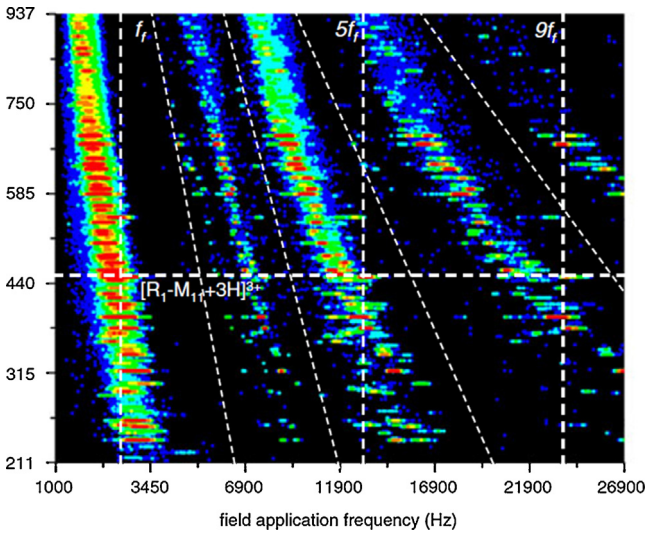

Fig. 17. OMS–MS spectrum of a tryptic digest of hemoglobin, myoglobin, cytochrome *c* doped with substance P using a four-phase wavedriver and showing increased resolving power with increased overtone. Bands can be seen for overtones, demonstrating the increased resolving power with higher overtones as well as the need for selection of overtones due to possible overlap.

Adapted from Ref. [230] with kind permission from Springer Science and Business Media.

the resolving power. One method of overcoming the practical constraints on length is to send ions around a circular drift tube, but circular drift tubes cannot use a static electric field to push ions around the circle as the ions will eventually reach the minimum of the electrical potential, travel to the lowest potential lenses, and be neutralized. To obtain cyclic motion the electric field is varied with the motion of the ions to ensure that they can always be driven around the circle. The two primary methods used to accomplish this vary the electric fields in the manner of OMS [79,136,223], shown in Fig. 18 and TWIMS [224]. Resolving powers of over 1000 [136] (examples of mixtures at lower resolving powers shown in Fig. 19) and 200 [139] have been reported for the two methods respectively.

One major complication with circular drift tubes arises from the possibility of high mobility ions lapping low mobility ions. If ion A travels twice as fast as ion B, then ion A will travel two cycles around the circle in the time it takes ion B to travel one cycle, and both will be at the same point in space. OMS methods have eliminated this by the use of an elimination region and having such a long elimination region that no overtones are produced. Only ions whose mobility matches the frequency of the applied fields transit the circular drift tube. As a selective technique, the first circular drift tube operated in an OMS-like mode avoids the challenges of faster ions lapping slower ions. The newer TWIMS circular drift tube operates in a dispersive mode and thus runs into this challenge. Originally the TWIMS circular drift tube was primarily operated by using only a narrow window of ejection from the circular drift tube, which limits the overall mobility range, but new modes of operation include the possible use of a ringdown mode [139,225] to obtain a series of peaks from which the mobilities can be determined via deconvolution from the repeating pattern to obtain mobilities.

Unlike most other selective techniques, circular drift tubes require the trapping of ions to accumulate them before injection into the drift tube. As a result, the advantages that would be gained by passing all ions from the source through the instrument, instead of accumulating ions, are mitigated. Instead, a new advance in circular drift tubes is the possibility of zoom mode ion mobility spectrometry. Zoom mode operation of circular drift tubes as

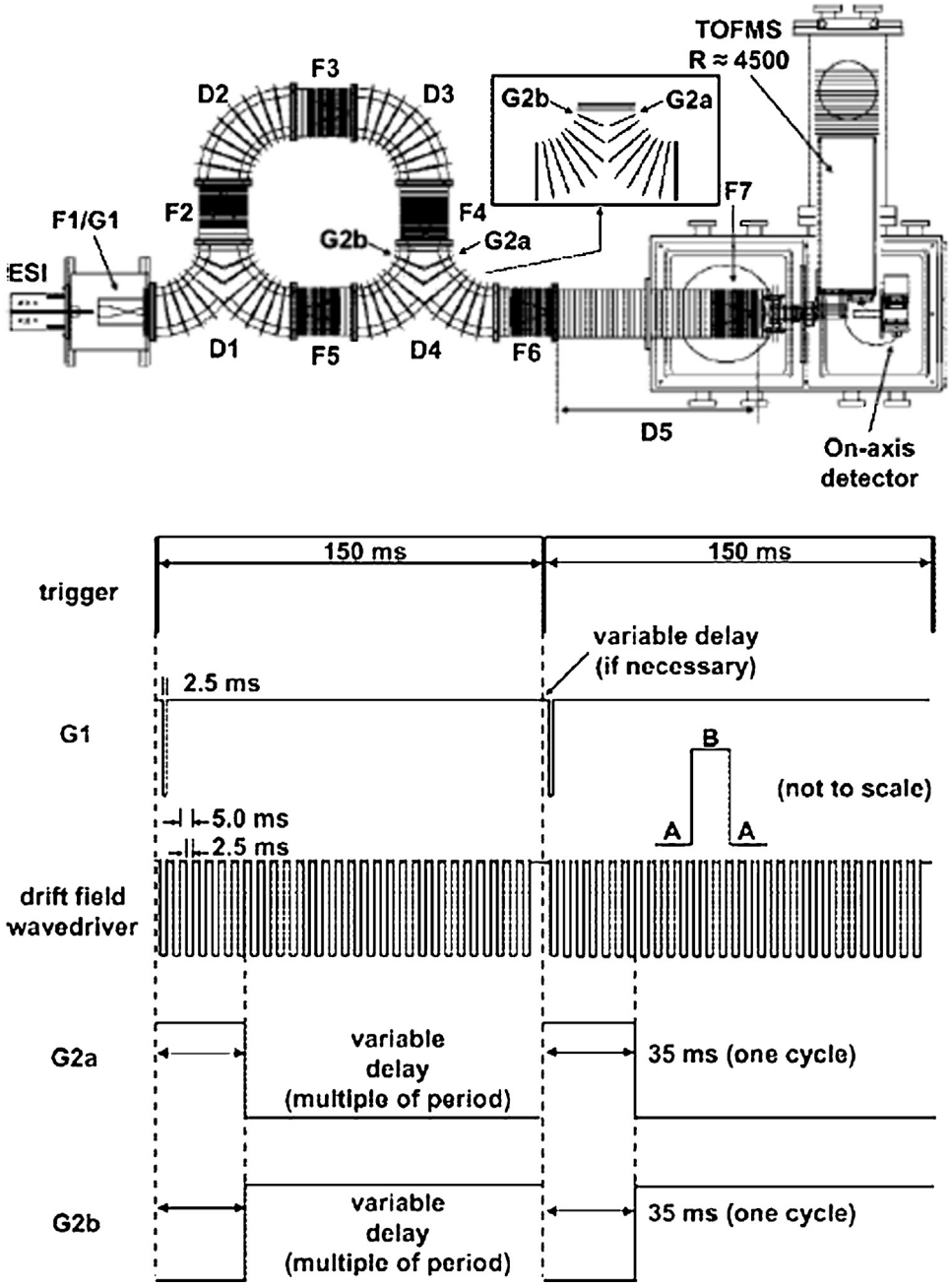

Fig. 18. Schematic of circular drift tube operated in OMS-like mode. Ions are generated by ESI, accumulated in funnel F1 before being gated into the circular drift tube via gate G1. The wavedriver is alternated between phases to propagate ions around the circular drift tube. In the conventional mode, gate 2 is alternated between open going around the circular drift tube one more time (G2b open) and directing ions into the TOF (G2a open).

Reprinted with permission from S.I. Merenbloom, R.S. Glaskin, Z.B. Henson, D.E. Clemmer, High-resolution ion cyclotron mobility spectrometry, Anal. Chem., 81 (2009) 1482–1487. Copyright 2009 American Chemical Society [79].

shown in Fig. 20 uses a circular drift tube orthogonal (and possibly but not necessarily overlapping) to a linear drift tube. Ions can either traverse a single pass of the linear drift tube in a dispersive DTIMS–MS or TWIMS–MS experiment or be injected into the circular drift tube and then pass as many times as desired around the circular drift tube. This allows a low resolution mode in a shorter time using the linear drift tube (operated in DTIMS or TWIMS mode) or a higher resolution mode that takes longer for analysis (operated in OMS or TWIMS mode), as befits the needs of the experiment. Furthermore, zoom mode allows targeting of the high resolution analysis to only those parts of the spectrum that is of interest, with a lower resolution for the complete dispersive mode IMS–MS spectrum.

2.2.6. Transversal modulation ion mobility spectrometry–mass spectrometry

TM-IMS is a new technique [80,174,226,227] that operates by using a single oscillating orthogonal (to the trajectory of net ion motion) electric field to determine whether ions transmit from the entrance slit to the exit slit or instead miss the exit slit and are neutralized as demonstrated in Fig. 21. Ions follow an axial electric field from the entrance slit to the exit slit and deviate from this trajectory on the basis of the orthogonal (deflector) field. Only ions that transit the device at an integer multiple of the oscillation period of the deflector field will exit through the exit slit. The oscillation frequency of the deflector field can then be scanned to obtain a mobility spectrum. Overtones are observed in TM-IMS-integer

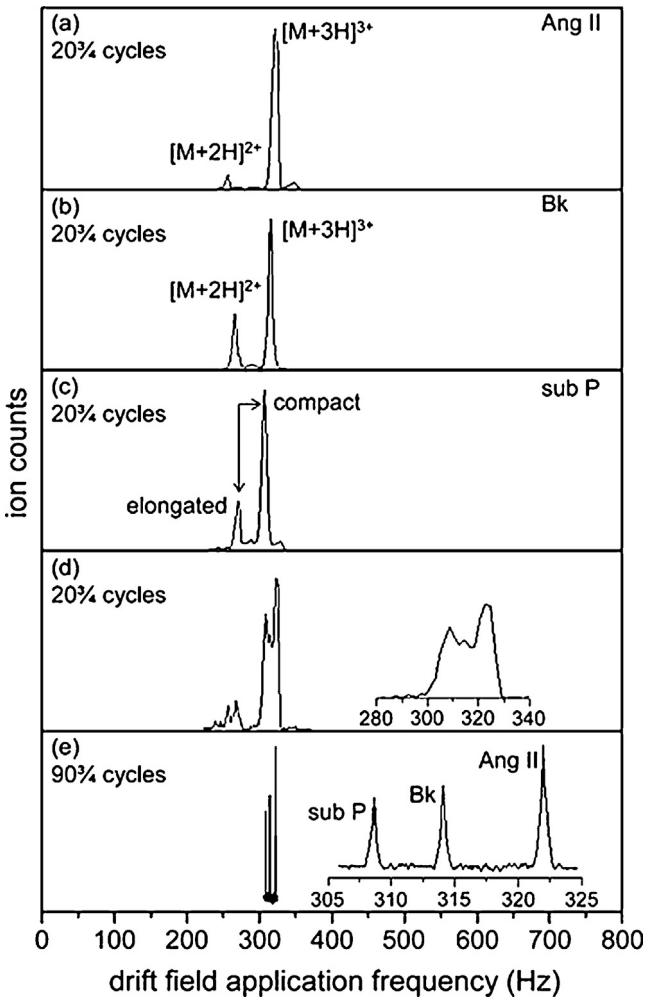

Fig. 19. Spectra from a circular drift tube experiment. Individual spectra of angiotensin II (Ang II), bradykinin (BK), and substance P (sub P) at 20 cycles around the circle along with a mixture showing incomplete separation at 20.75 cycles and very high resolution at 90.75 cycles. Drift field application frequency is inversely proportional to mobility.

Reprinted with permission from R.S. Glaskin, M.A. Ewing, D.E. Clemmer, Ion trapping for ion mobility spectrometry measurements in a cyclical drift tube, Anal. Chem., 85 (2013) 7003–7008. Copyright 2013 American Chemical Society [136].

multiples of the fundamental deflector oscillation frequency also transmit ions of the same mobility and thus we expect species of significantly different mobilities to overlap in frequency. Because the oscillating field is restorative in nature, bringing ions back to a

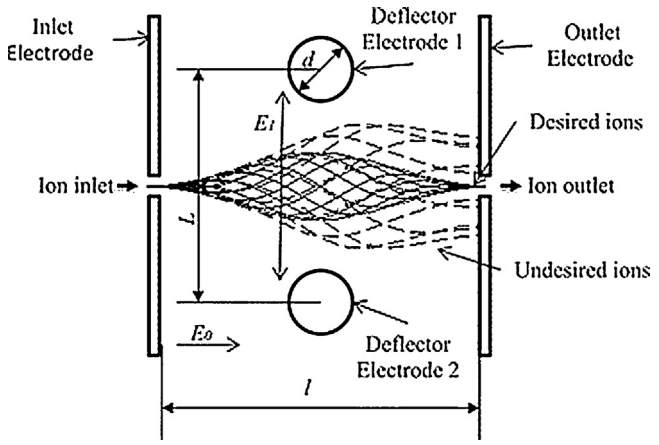

Fig. 21. Method of separation of ions in TM-IMS. Ions who feel the effect of the deflector field for an integer cycle of the deflector field exit the ion outlet while ions that feel it for a non-integer cycle collide with the outlet electrode and are lost.

Reprinted from the International Journal of Mass Spectrometry, 376, César Barrios-Collado, Guillermo Vidal-de-Miguel, Numerical algorithm for the accurate evaluation of ion beams in transversal modulation ion mobility spectrometry: Understanding realistic geometries, 97–105, 2015, with permission from Elsevier [227].

central path, instead of eliminating as in OMS, it does not appear that the same method used to select overtones in OMS can be used to select overtones in TM-IMS, but we remain hopeful that such spectral simplification can be obtained. Because the selection is by way of an orthogonal electric field, turning off the field should result in transmission of ions of all mobilities. Unfortunately the selection is not complete as unselected ions can still exit the device in bursts as their path crosses the exit slit and result in some background [80,174]; however, these bursts or pulses of unselected ions can be eliminated through the use of a dual-stage TM-IMS device [174] and as shown in Fig. 22.

Despite the young age of this technique, shown especially by achieved resolving powers of ~60 [174,227], its many interesting characteristics show promise. In many ways they resemble those of a DMA instrument: a constant flow of mobility selected ions through a high pressure device. The constant flow is ideal for experiments where a maximum flow of a mobility selected ion is desired and the high pressure offers advantages in the coupling to ion generation at atmospheric pressure. TM-IMS instruments are typically operated in the low-field regime due to the high pressure, and the concerns about the stability of gas-flow are eliminated in TM-IMS where the flux of gas is not so high as to often result in turbidity. By moving away from a high flux of gas, TM-IMS instruments

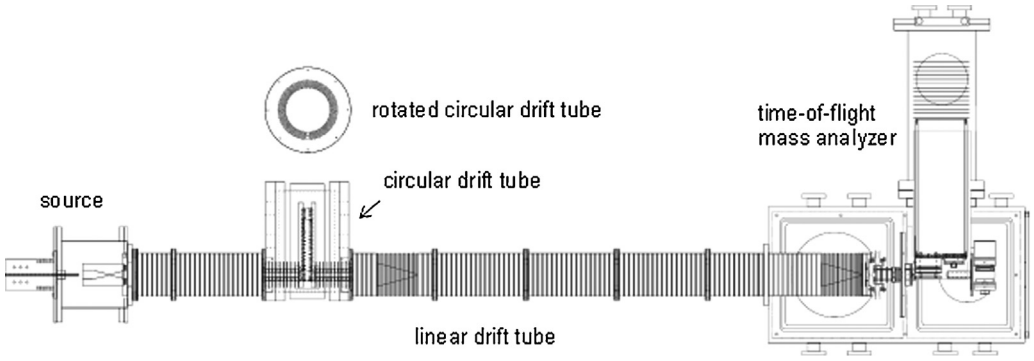

Fig. 20. Schematic of an instrument for zoom mode ion mobility spectrometry with a source on the left, a linear drift tube down the center and a time-of-flight mass analyzer on the right. Interrupting the linear drift tube is a chamber containing a circular drift tube orthogonal to the ion trajectory through the linear drift tube and out of the plane of the schematic. The circular drift tube is shown rotated into the plane of the schematic above its location within the instrument. Ions can propagate through the linear drift tube or be directed into the circular drift tube dependent upon the voltages applied to the lenses at the interface.

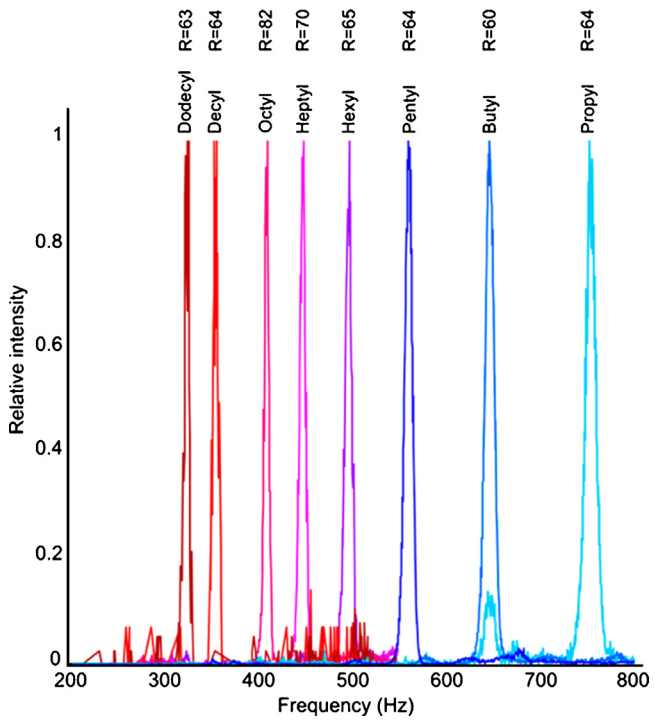

Fig. 22. TM-IMS spectra of different tetraalkylammonium ions measured at different *m/z* selections in a quadrupole after TM-IMS separation showing good separation and very little background on a tandem IMS–IMS instrument.

Reprinted with permission from G. Vidal-de-Miguel, M. Macía, C. Barrios, J. Cuevas, Transversal modulation ion mobility spectrometry (IMS) coupled with mass spectrometry (MS): exploring the IMS–IMS–MS possibilities of the instrument, Anal. Chem., 87 (2015) 1925–1932. Copyright 2015 American Chemical Society [174].

should be operable at a range of pressures depending upon application, and also avoid the difficulties in engineering high resolution devices while avoiding turbidity due to small irregularities in surface. Similar to other slit-based instruments such as FAIMS and DMA, TM-IMS resolving power is in part limited by the slit width, and narrowing the slit should increase the resolving power but at a cost to signal. As with most mobility separation techniques, increasing the electric field, in particular the deflector field, can be used to increase the resolving power, but at the cost of moving out of the low-field regime and possible electrical breakdown. Unlike OMS, TM-IMS does not appear to lead to increased resolving power at higher overtones but at the same time signal does not decrease with higher overtones, thus selection would be ideal to reduce overlap of peaks but should not effect resolving power nor reduce signal. At present TM-IMS has been coupled to a triple quadrupole [174] and a linear ion trap [174], but we expect more couplings in the future.

3. Conclusions

In this review we have discussed the past, present, and future of current mobility separation techniques, from the nesting of IMS and MS to the new techniques of TIMS and TM-IMS. Most of the instrumentation advances of the last two decades have come in increased IMS sensitivity through an improved coupling to ion generation and mass spectrometers. One of the key current bottlenecks in improving hybrid IMS–MS instrumentation is an improvement in IMS resolution, with very few advances since the turn of the century. An order of magnitude improvement in resolving power would revolutionize the field, transforming IMS into a technique that could regularly separate protomers, ions that differ only in the location of a proton [228]; isotopologues, ions that differ only in isotopic composition, in a method that could result in an internal mass scale [229]; and isotopomers, ions that differ only by the location of different isotopes [215]. With the multitude of new techniques and technologies under development, there is significant hope for a major breakthrough in resolution which promises to fundamentally change our understanding of structure, in a manner analogous to how high resolution mass spectrometry has enabled a wide range of new experiments. Among the few areas where sensitivity is still a significant bottleneck is circular (or very long path-length) drift tubes, where a design centered around structures for lossless ion manipulation [152–155] or a similar technology might assist in ion transmission and manipulation and thus enable increased separation capacity.

Acknowledgements

The authors would like to thank Indiana University for financial support during manuscript preparation and all the funding institutions that have funded them over the many years with which they have worked in this field and the members of the community for insightful and enlightening interactions.

References

[1] H.E. Revercomb, E.A. Mason, Theory of plasma chromatography gaseous electrophoresis – review, Anal. Chem. 47 (1975) 970–983.
[2] G. von Helden, M.T. Hsu, N. Gotts, M.T. Bowers, Carbon cluster cations with up to 84 atoms – structures, formation mechanism, and reactivity, J. Phys. Chem. 97 (1993) 8182–8192.
[3] G. von Helden, T. Wyttenbach, M.T. Bowers, Inclusion of a MALDI ion-source in the ion chromatography technique – conformational information on polymer and biomolecular ions, Int. J. Mass Spectrom. Ion Process. 146 (1995) 349–364.
[4] T. Wyttenbach, G. von Helden, M.T. Bowers, Gas-phase conformation of biological molecules: bradykinin, J. Am. Chem. Soc. 118 (1996) 8355–8364.
[5] R.H. St Louis, H.H.J. Hill, G.A. Eiceman, Ion mobility spectrometry in analytical chemistry, Crit. Rev. Anal. Chem. 21 (1990) 321–356.
[6] G. von Helden, N.G. Gotts, M.T. Bowers, Experimental-evidence for the formation of fullerenes by collisional heating of carbon rings in the gas-phase, Nature 363 (1993) 60–63.
[7] G. von Helden, M.T. Hsu, N.G. Gotts, P.R. Kemper, M.T. Bowers, Do small fullerenes exist only on the computer – experimental results on $C_{20}^{+/-}$ and $C_{24}^{+/-}$, Chem. Phys. Lett. 204 (1993) 15–22.
[8] J.M. Hunter, J.L. Fye, M.F. Jarrold, Annealing and dissociation of carbon rings, J. Chem. Phys. 99 (1993) 1785–1795.
[9] J. Hunter, J. Fye, M.F. Jarrold, Annealing C_{60}^{+}: synthesis of fullerenes and large carbon rings, Science 260 (1993) 784–786.
[10] J. Hunter, J. Fye, M.F. Jarrold, Carbon rings, J. Phys. Chem. 97 (1993) 3460–3462.
[11] J.M. Hunter, J.L. Fye, E.J. Roskamp, M.F. Jarrold, Annealing carbon cluster ions: a mechanism for fullerene synthesis, J. Phys. Chem. 98 (1994) 1810–1818.
[12] M. Zhou, N. Morgner, N.P. Barrera, A. Politis, S.C. Isaacson, D. Matak-Vinkovic, T. Murata, R.A. Bernal, D. Stock, C.V. Robinson, Mass spectrometry of intact V-type ATPases reveals bound lipids and the effects of nucleotide binding, Science 334 (2011) 380–385.
[13] M. Zhou, A. Politis, R.B. Davies, I. Liko, K.-J. Wu, A.G. Stewart, D. Stock, C.V. Robinson, Mass spectrometry of intact V-type ATPases reveals bound lipids and the effects of nucleotide binding, Nat. Chem. 6 (2014) 208–215.
[14] C.A. Srebalus, J.W. Li, W.S. Marshall, D.E. Clemmer, Gas phase separations of electrosprayed peptide libraries, Anal. Chem. 71 (1999) 3918–3927.
[15] Y.J. Lee, C.S. Hoaglund-Hyzer, C.A. Srebalus Barnes, A.E. Hilderbrand, S.J. Valentine, D.E. Clemmer, Development of high-throughput LC-injected ion mobility-Q-TOF techniques for analysis of complex peptide mixtures, J. Chromatogr. B 782 (2002) 343–351.
[16] C.A. Srebalus Barnes, A.E. Hilderbrand, S.J. Valentine, D.E. Clemmer, Resolving isomeric peptide mixtures: a combined HPLC/ion mobility-TOFMS analysis of a 4000-component combinatorial library, Anal. Chem. 74 (2002) 26–36.
[17] R. Guevremont, D.A. Barnett, R.W. Purves, J. Vandermey, Analysis of a tryptic digest of pig hemoglobin using ESI-FAIMS–MS, Anal. Chem. 72 (2000) 4577–4584.
[18] S. Myung, Y.J. Lee, M.H. Moon, J.A. Taraszka, R. Sowell, S.L. Koeniger, A.E. Hilderbrand, S.J. Valentine, L. Cherbas, P. Cherbas, T.C. Kaufmann, D.F. Miller, Y. Mechref, M.V. Novotny, M.A. Ewing, D.E. Clemmer, Development of high-sensitivity ion trap-IMS-TOF techniques: a high-throughput nano-LC/IMS/TOF separation of the Drosophila fly proteome, Anal. Chem. 75 (2003) 5137–5145.
[19] E.N. Nikolaev, A. Shukla, C. Masselon, S. Sharma, L. Pasa-Tolic, R. Smith, Combination of field asymmetric ion mobility spectrometry (FAIMS) with FT ICR mass spectrometry for proteomics research, Mol. Cell. Proteomics 3 (2004) S136.

[20] S.J. Valentine, X. Liu, M.D. Plasencia, A.E. Hilderbrand, R.T. Kurulugama, S.L. Koeniger, D.E. Clemmer, Developing liquid chromatography ion mobility mass spectrometry techniques, Expert Rev. Proteomics 2 (2005) 553–565.
[21] S.J. Valentine, M.D. Plasencia, X. Liu, M. Krishnan, S. Naylor, H.R. Udseth, R.D. Smith, D.E. Clemmer, Toward plasma proteome profiling with ion mobility-mass spectrometry, J. Proteome Res. 5 (2006) 2977–2984.
[22] A.A. Shvartsburg, K. Tang, R.D. Smith, Two-dimensional ion mobility analyses of proteins and peptides, in: M.S. Lipton, P.T. Ljiljana (Eds.), Methods in Molecular Biology, 2009, pp. 417–445.
[23] E.S. Baker, E.A. Livesay, D.J. Orton, R.J. Moore, W.F. Danielson, D.C. Prior 3rd, Y.M. Ibrahim, B.L. LaMarche, A.M. Mayampurath, A.A. Schepmoes, D.F. Hopkins, K. Tang, R.D. Smith, M.E. Belov, An LC–IMS–MS platform providing increased dynamic range for high-throughput proteomic studies, J. Proteome Res. 9 (2010) 997–1006.
[24] K. Blackburn, F. Mbeunkui, S.K. Mitra, T. Mentzel, M.B. Goshe, Improving protein and proteome coverage through data-independent multiplexed peptide fragmentation, J. Proteome Res. 9 (2010) 3621–3637.
[25] P.V. Shliaha, N.J. Bond, L. Gatto, K.S. Lilley, Effects of traveling wave ion mobility separation on data independent acquisition in proteomics studies, J. Proteome Res. 12 (2013) 2323–2339.
[26] G.C. Donohoe, H. Maleki, J.R. Arndt, M. Khakinejad, J.H. Yi, C. McBride, T.R. Nurkiewicz, S.J. Valentine, A new ion mobility-linear ion trap instrument for complex mixture analysis, Anal. Chem. 86 (2014) 8121–8128.
[27] U. Distler, J. Kuharev, P. Navarro, Y. Levin, H. Schild, S. Tenzer, Drift time-specific collision energies enable deep-coverage data-independent acquisition proteomics, Nat. Methods 11 (2014) 167–170.
[28] M.H. Moon, S. Myung, M. Plasencia, A.E. Hilderbrand, D.E. Clemmer, Nanoflow LC/ion mobility/CID/TOF for proteomics: analysis of a human urinary proteome, J. Proteome Res. 2 (2003) 589–597.
[29] N.F. Zinnel, P.-J. Pai, D.H. Russell, Ion mobility-mass spectrometry (IM-MS) for top-down proteomics: increased dynamic range affords increased sequence coverage, Anal. Chem. 84 (2012) 3390–3397.
[30] X. Guo, E. Lankmayr, Multidimensional approaches in LC and MS for phospholipid bioanalysis, Bioanalysis 2 (2010) 1109–1123.
[31] K. Kaplan, P. Dwivedi, S. Davidson, Q. Yang, P. Tso, W. Siems, H.H. Hill Jr., Monitoring dynamic changes in lymph metabolome of fasting and fed rats by electrospray ionization-ion mobility mass spectrometry (ESI-IMMS), Anal. Chem. 81 (2009) 7944–7953.
[32] C.S. Hoaglund-Hyzer, J.W. Li, D.E. Clemmer, Mobility labeling for parallel CID of ion mixtures, Anal. Chem. 72 (2000) 2737–2740.
[33] Y.J. Lee, C.S. Hoaglund-Hyzer, J.A. Taraszka, G.A. Zientara, A.E. Counterman, D.E. Clemmer, Collision-induced dissociation of mobility-separated ions using an orifice-skimmer cone at the back of a drift tube, Anal. Chem. 73 (2001) 3549–3555.
[34] C.S. Hoaglund-Hyzer, D.E. Clemmer, Ion trap/ion mobility/quadrupole/time of flight mass spectrometry for peptide mixture analysis, Anal. Chem. 73 (2001) 177–184.
[35] C.S. Hoaglund-Hyzer, Y.J. Lee, A.E. Counterman, D.E. Clemmer, Coupling ion mobility separations, collisional activation techniques, and multiple stages of MS for analysis of complex peptide mixtures, Anal. Chem. 74 (2002) 992–1006.
[36] S.J. Valentine, S.L. Koeniger, D.E. Clemmer, A split-field drift tube for separation and efficient fragmentation of biomolecular ions, Anal. Chem. 75 (2003) 6202–6208.
[37] S.L. Koeniger, S.J. Valentine, S. Myung, M. Plasencia, Y.J. Lee, D.E. Clemmer, Development of field modulation in a split-field drift tube for high-throughput multidimensional separations, J. Proteome Res. 4 (2005) 25–35.
[38] S.J. Valentine, S. Sevugarajan, R.T. Kurulugama, S.L. Koeniger, S.I. Merenbloom, B.C. Bohrer, D.E. Clemmer, Split-field drift tube/mass spectrometry and isotopic labeling techniques for determination of single amino acid polymorphisms, J. Proteome Res. 5 (2006) 1879–1887.
[39] X. Liu, S.J. Valentine, M.D. Plasencia, S. Trimpin, S. Naylor, D.E. Clemmer, Mapping the human plasma proteome by SCX-LC–IMS–MS, J. Am. Soc. Mass Spectrom. 18 (2007) 1249–1264.
[40] D. Isailovic, R.T. Kurulugama, M.D. Plasencia, S.T. Stokes, Z. Kyselova, R. Goldman, Y. Mechref, M.V. Novotny, D.E. Clemmer, Profiling of human serum glycans associated with liver cancer and cirrhosis by IMS–MS, J. Proteome Res. 7 (2008) 1109–1117.
[41] D. Isailovic, M.D. Plasencia, M.M. Gaye, S.T. Stokes, R.T. Kurulugama, V. Pungpapong, M. Zhang, Z. Kyselova, R. Goldman, Y. Mechref, M.V. Novotny, D.E. Clemmer, Delineating diseases by IMS–MS profiling of serum N-linked glycans, J. Proteome Res. 11 (2012) 576–585.
[42] M.M. Gaye, S.J. Valentine, Y. Hu, N. Mirjankar, Z.T. Hammoud, Y. Mechref, B.K. Lavine, D.E. Clemmer, Ion mobility-mass spectrometry analysis of serum N-linked glycans from esophageal adenocarcinoma phenotypes, J. Proteome Res. 11 (2012) 6102–6110.
[43] S.J. Valentine, A.E. Counterman, C.S. Hoaglund-Hyzer, D.E. Clemmer, Intrinsic amino acid size parameters from a series of 113 lysine-terminated tryptic digest peptide ions, J. Phys. Chem. B 103 (1999) 1203–1207.
[44] A.A. Shvartsburg, K.W.M. Siu, D.E. Clemmer, Prediction of peptide ion mobilities via a priori calculations from intrinsic size parameters of amino acid residues, J. Am. Soc. Mass Spectrom. 12 (2001) 885–888.
[45] S.J. Valentine, M.A. Ewing, J.M. Dilger, M.S. Glover, S. Geromanos, C. Hughes, D.E. Clemmer, Using ion mobility data to improve peptide identification: intrinsic amino acid size parameters, J. Proteome Res. 10 (2011) 2318–2329.
[46] C. Becker, F.A. Fernandez-Lima, D.H. Russell, Ion mobility-mass spectrometry: a tool for characterizing the petroleome, Spectroscopy 24 (2009) 38–42.
[47] Z. Li, S.J. Valentine, D.E. Clemmer, Complexation of amino compounds by 18c6 improves selectivity by IMS–IMS–MS: application to petroleum characterization, J. Am. Soc. Mass Spectrom. 22 (2011) 817–827.
[48] S. Trimpin, M. Plasencia, D. Isailovic, D.E. Clemmer, Resolving oligomers from fully grown polymers with IMS–MS, Anal. Chem. 79 (2007) 7965–7974.
[49] J.N. Hoskins, S. Trimpin, S.M. Grayson, Architectural differentiation of linear and cyclic polymeric isomers by ion mobility spectrometry–mass spectrometry, Macromolecules 44 (2011) 6915–6918.
[50] T.J. El-Baba, C.A. Lutomski, B. Wang, S. Trimpin, Characterizing synthetic polymers and additives using new ionization methods for mass spectrometry, Rapid Commun. Mass Spectrom. 28 (2014) 1175–1184.
[51] C. Larriba, J.F. de la Mora, D.E. Clemmer, Electrospray ionization mechanisms for large polyethylene glycol chains studied through tandem ion mobility spectrometry, J. Am. Soc. Mass Spectrom. 25 (2014) 1332–1345.
[52] E. Mack, Average cross-sectional areas of molecules by gaseous diffusion methods, J. Am. Chem. Soc. 47 (1925) 2468–2482.
[53] M.F. Jarrold, V.A. Constant, Silicon cluster ions: evidence for a structural transition, Phys. Rev. Lett. 67 (1991) 2994–2997.
[54] D.E. Clemmer, J.M. Hunter, K.B. Shelimov, M.F. Jarrold, Physical and chemical evidence for metallofullerenes with metal atoms as part of the cage, Nature 372 (1994) 248–250.
[55] A.A. Shvartsburg, M.F. Jarrold, An exact hard-spheres scattering model for the mobilities of polyatomic ions, Chem. Phys. Lett. 261 (1996) 86–91.
[56] M.F. Mesleh, J.M. Hunter, A.A. Shvartsburg, G.C. Schatz, M.F. Jarrold, Structural information from ion mobility measurements: effects of the long-range potential, J. Phys. Chem. 100 (1996) 16082–16086.
[57] M.F. Mesleh, J.M. Hunter, A.A. Shvartsburg, G.C. Schatz, M.F. Jarrold, Structural information from ion mobility measurements: effects of the long-range potential, J. Phys. Chem. A 101 (1997) 968.
[58] D.E. Clemmer, M.F. Jarrold, Ion mobility measurements and their applications to clusters and biomolecules, J. Mass Spectrom. 32 (1997) 577–592.
[59] D. Wittmer, B.K. Luckenbill, H.H. Hill, Y.H. Chen, Electrospray-ionization ion mobility spectrometry, Anal. Chem. 66 (1994) 2348–2355.
[60] K.B. McAfee, D. Edelson, Identification and mobility of ions in a townsend discharge by time-resolved mass spectrometry, Proc. Phys. Soc. Lond. 81 (1963) 382–384.
[61] C.E. Young, D. Edelson, W.E. Falconer, Water cluster ions – rates of formation and decomposition of hydrates of hydronium ion, J. Chem. Phys. 53 (1970) 4295–4302.
[62] L.G. McKnight, K.B. McAfee, D.P. Sipler, Low-field drift velocities and reactions of nitrogen ions in nitrogen, Phys. Rev. 164 (1967) 62–70.
[63] W.S. Barnes, D.W. Martin, E.W. McDaniel, Mass spectrographic identification of ion observed in hydrogen mobility experiments, Phys. Rev. Lett. 6 (1961) 110–111.
[64] E.W. McDaniel, W.S. Barnes, D.W. Martin, Drift tube-mass spectrometer for studies of low-energy ion-molecule reactions, Rev. Sci. Instrum. 33 (1962) 2–7.
[65] C.S. Hoaglund, S.J. Valentine, C.R. Sporleder, J.P. Reilly, D.E. Clemmer, Three-dimensional ion mobility TOFMS analysis of electrosprayed biomolecules, Anal. Chem. 70 (1998) 2236–2242.
[66] K. Giles, S.D. Pringle, K.R. Worthington, D. Little, J.L. Wildgoose, R.H. Bateman, Applications of a travelling wave-based radio-frequency-only stacked ring ion guide, Rapid Commun. Mass Spectrom. 18 (2004) 2401–2414.
[67] K. Thalassinos, S.E. Slade, K.R. Jennings, J.H. Scrivens, K. Giles, J. Wildgoose, J. Hoyes, R.H. Bateman, M.T. Bowers, Ion mobility mass spectrometry of proteins in a modified commercial mass spectrometer, Int. J. Mass Spectrom. 236 (2004) 55–63.
[68] F.A. Fernandez-Lima, D.A. Kaplan, M.A. Park, Note: Integration of trapped ion mobility spectrometry with mass spectrometry, Rev. Sci. Instrum. 82 (2011) 126106.
[69] F. Fernandez-Lima, D.A. Kaplan, J. Suetering, M.A. Park, Gas-phase separation using a trapped ion mobility spectrometer, Int. J. Ion Mobil. Spectrom. 14 (2011) 93–98.
[70] J. Rosell-Llompart, I.G. Loscertales, D. Bingham, J. Fernández de la Mora, Sizing nanoparticles and ions with a short differential mobility analyzer, J. Aerosol Sci. 27 (1996) 695–719.
[71] J.F. de la Mora, S. Ude, B.A. Thomson, The potential of differential mobility analysis coupled to MS for the study of very large singly and multiply charged proteins and protein complexes in the gas phase, Biotechnol. J. 1 (2006) 988–997.
[72] J. Rus, D. Moro, J.A. Sillero, J. Royuela, A. Casado, F. Estevez-Molinero, J. Fernández de la Mora, IMS–MS studies based on coupling a differential mobility analyzer (DMA) to commercial API–MS systems, Int. J. Mass Spectrom. 298 (2010) 30–40.
[73] S.L. Kaufman, J.W. Skogen, F.D. Dorman, F. Zarrin, K.C. Lewis, Macromolecule analysis based on electrophoretic mobility in air: globular proteins, Anal. Chem. 68 (1996) 1895–1904.
[74] S.L. Kaufman, J.W. Skogen, F.D. Dorman, F. Zarrin, K.C. Lewis, Macromolecule analysis based on electrophoretic mobility in air: globular proteins, Anal. Chem. 68 (1996) 3703.
[75] R. Guevremont, K.W.M. Siu, J.Y. Wang, L.Y. Ding, Combined ion mobility time-of-flight mass spectrometry study of electrospray-generated ions, Anal. Chem. 69 (1997) 3959–3965.

[76] R.W. Purves, R. Guevremont, S. Day, C.W. Pipich, M.S. Matyjaszczyk, Mass spectrometric characterization of a high-field asymmetric waveform ion mobility spectrometer, Rev. Sci. Instrum. 69 (1998) 4094–4105.
[77] S.J. Valentine, S.T. Stokes, R.T. Kurulugama, F.M. Nachtigall, D.E. Clemmer, Overtone mobility spectrometry: Part 2. Theoretical considerations of resolving power, J. Am. Soc. Mass Spectrom. 20 (2009) 738–750.
[78] R.T. Kurulugama, F.M. Nachtigall, S. Lee, S.J. Valentine, D.E. Clemmer, Overtone mobility spectrometry: Part 1. Experimental observations, J. Am. Soc. Mass Spectrom. 20 (2009) 729–737.
[79] S.I. Merenbloom, R.S. Glaskin, Z.B. Henson, D.E. Clemmer, High-resolution ion cyclotron mobility spectrometry, Anal. Chem. 81 (2009) 1482–1487.
[80] G. Vidal-de-Miguel, M. Macía, J. Cuevas, Transversal modulation ion mobility spectrometry (TM-IMS), a new mobility filter overcoming turbulence related limitations, Anal. Chem. 84 (2012) 7831–7837.
[81] E.A. Mason, E.W. McDaniel, Transport Properties of Ions in Gases, WILEY-VCH Verlag GmbH & Co. KGaA, Weinheim, Federal Republic of Germany, 1988.
[82] E. Rutherford, The velocity and rate of recombination of the ions of gases exposed to Röntgen radiation, Philos. Mag. Ser. 5 (44) (1897) 422–440.
[83] J. Zeleny, On the ratio of the velocities of the two ions produced in gases by Röntgen radiation; and on some related phenomena, Philos. Mag. Ser. 5 (46) (1898) 120–154.
[84] J.J. Thomson, Cathode rays, Philos. Mag. Ser. 5 (44) (1897) 293–316.
[85] C. Bleiholder, T. Wyttenbach, M.T. Bowers, A novel projection approximation algorithm for the fast and accurate computation of molecular collision cross sections (I). Method, Int. J. Mass Spectrom. 308 (2011) 1–10.
[86] C. Bleiholder, S. Contreras, T.D. Do, M.T. Bowers, A novel projection approximation algorithm for the fast and accurate computation of molecular collision cross sections (II). Model parameterization and definition of empirical shape factors for proteins, Int. J. Mass Spectrom. 345 (2013) 89–96.
[87] C. Bleiholder, S. Contreras, M.T. Bowers, A novel projection approximation algorithm for the fast and accurate computation of molecular collision cross sections (IV). Application to polypeptides, Int. J. Mass Spectrom. 354 (2013) 275–280.
[88] S.E. Anderson, C. Bleiholder, E.R. Brocker, P.J. Stang, M.T. Bowers, A novel projection approximation algorithm for the fast and accurate computation of molecular collision cross sections (III): Application to supramolecular coordination-driven assemblies with complex shapes, Int. J. Mass Spectrom. 330 (2012) 78–84.
[89] A.A. Shvartsburg, B. Liu, K.W.M. Siu, K.M. Ho, Evaluation of ionic mobilities by coupling the scattering on atoms and on electron density, J. Phys. Chem. A 104 (2000) 6152–6157.
[90] A.A. Shvartsburg, B. Liu, M.F. Jarrold, K.M. Ho, Modeling ionic mobilities by scattering on electronic density isosurfaces: application to silicon cluster anions, J. Chem. Phys. 112 (2000) 4517–4526.
[91] Y. Alexeev, D.G. Fedorov, A.A. Shvartsburg, Effective ion mobility calculations for macromolecules by scattering on electron clouds, J. Phys. Chem. A 118 (2014) 6763–6772.
[92] G.R. Asbury, H.H. Hill, Using different drift gases to change separation factors (alpha) in ion mobility spectrometry, Anal. Chem. 72 (2000) 580–584.
[93] L.W. Beegle, I. Kanik, L. Matz, H.H. Hill, Effects of drift-gas polarizability on glycine peptides in ion mobility spectrometry, Int. J. Mass Spectrom. 216 (2002) 257–268.
[94] L.M. Matz, H.H. Hill, L.W. Beegle, I. Kanik, Investigation of drift gas selectivity in high resolution ion mobility spectrometry with mass spectrometry detection, J. Am. Soc. Mass Spectrom. 13 (2002) 300–307.
[95] B.T. Ruotolo, J.A. McLean, K.J. Gillig, D.H. Russell, The influence and utility of varying field strength for the separation of tryptic peptides by ion mobility-mass spectrometry, J. Am. Soc. Mass Spectrom. 16 (2005) 158–165.
[96] M.F. Bush, Z. Hall, K. Giles, J. Hoyes, C.V. Robinson, B.T. Ruotolo, Collision cross sections of proteins and their complexes: a calibration framework and database for gas-phase structural biology, Anal. Chem. 82 (2010) 9557–9565.
[97] M.F. Bush, I.D.G. Campuzano, C.V. Robinson, Ion mobility mass spectrometry of peptide ions: effects of drift gas and calibration strategies, Anal. Chem. 84 (2012) 7124–7130.
[98] C. Larriba-Andaluz, J. Fernández-García, M.A. Ewing, C.J. Hogan, D.E. Clemmer, Gas molecule scattering & ion mobility measurements for organic macroions in He versus N_2 environments, Phys. Chem. Chem. Phys. 17 (2015) 15019–15029.
[99] Y.S. Liu, S.J. Valentine, A.E. Counterman, C.S. Hoaglund, D.E. Clemmer, Injected-ion mobility analysis of biomolecules, Anal. Chem. 69 (1997) A728–A735.
[100] M. Kwasnik, K. Fuhrer, M. Gonin, K. Barbeau, F.M. Fernandez, Performance, resolving power, and radial ion distributions of a prototype nanoelectrospray ionization resistive glass atmospheric pressure ion mobility spectrometer, Anal. Chem. 79 (2007) 7782–7791.
[101] A.B. Kanu, M.M. Gribb, H.H. Hill, Predicting optimal resolving power for ambient pressure ion mobility spectrometry, Anal. Chem. 80 (2008) 6610–6619.
[102] F. Albrieux, F. Calvo, F. Chirot, A. Vorobyev, Y.O. Tsybin, V. Lepere, R. Antoine, J. Lemoine, P. Dugourd, Conformation of polyalanine and polyglycine dications in the gas phase: insight from ion mobility spectrometry and replica-exchange molecular dynamics, J. Phys. Chem. A 114 (2010) 6888–6896.
[103] R.C. Blase, J.A. Silveira, K.J. Gillig, C.M. Gamage, D.H. Russell, Increased ion transmission in IMS: a high resolution, periodic-focusing DC ion guide ion mobility spectrometer, Int. J. Mass Spectrom. 301 (2011) 166–173.
[104] S.M. Zucker, M.A. Ewing, D.E. Clemmer, Gridless overtone mobility spectrometry, Anal. Chem. 85 (2013) 10174–10179.
[105] K. Giles, J.P. Williams, I. Campuzano, Enhancements in travelling wave ion mobility resolution, Rapid Commun. Mass Spectrom. 25 (2011) 1559–1566.
[106] J.C. May, C.R. Goodwin, N.M. Lareau, K.L. Leaptrot, C.B. Morris, R.T. Kurulugama, A. Mordehai, C. Klein, W. Barry, E. Darland, G. Overney, K. Imatani, G.C. Stafford, J.C. Fjeldsted, J.A. McLean, Conformational ordering of biomolecules in the gas phase: nitrogen collision cross sections measured on a prototype high resolution drift tube ion mobility-mass spectrometer, Anal. Chem. 86 (2014) 2107–2116.
[107] C. Jia, C.B. Lietz, Q. Yu, L. Li, Site-specific characterization of D-amino acid containing peptide epimers by ion mobility spectrometry, Anal. Chem. 86 (2014) 2972–2981.
[108] S.C. Henderson, J.W. Li, A.E. Counterman, D.E. Clemmer, Intrinsic size parameters for Val, Ile, Leu, Gln, Thr, Phe, and Trp residues from ion mobility measurements of polyamino acid ions, J. Phys. Chem. B 103 (1999) 8780–8785.
[109] R. Salbo, M.F. Bush, H. Naver, I. Campuzano, C.V. Robinson, I. Pettersson, T.J.D. Jorgensen, K.F. Haselmann, Traveling-wave ion mobility mass spectrometry of protein complexes: accurate calibrated collision cross-sections of human insulin oligomers, Rapid Commun. Mass Spectrom. 26 (2012) 1181–1193.
[110] S.K. Chowdhury, V. Katta, B.T. Chait, Probing conformational-changes in proteins by mass-spectrometry, J. Am. Chem. Soc. 112 (1990) 9012–9013.
[111] J.A. Loo, C.G. Edmonds, H.R. Udseth, R.D. Smith, Effect of reducing disulfide-containing proteins on electrospray ionization mass-spectra, Anal. Chem. 62 (1990) 693–698.
[112] U.A. Mirza, S.L. Cohen, B.T. Chait, Heat-induced conformational-changes in proteins studied by electrospray ionization mass-spectrometry, Anal. Chem. 65 (1993) 1–6.
[113] R.R. Hudgins, J. Woenckhaus, M.F. Jarrold, High resolution ion mobility measurements for gas phase proteins: correlation between solution phase and gas phase conformations, Int. J. Mass Spectrom. 165 (1997) 497–507.
[114] A.J. Heck, Native mass spectrometry: a bridge between interactomics and structural biology, Nat. Methods 5 (2008) 927–933.
[115] L. Shi, A.E. Holliday, H. Shi, F. Zhu, M.A. Ewing, D.H. Russell, D.E. Clemmer, Characterizing intermediates along the transition from polyproline I to polyproline II using ion mobility spectrometry–mass spectrometry, J. Am. Chem. Soc. 136 (2014) 12702–12711.
[116] H. Shi, D.E. Clemmer, Evidence for two new solution states of ubiquitin by IMS–MS analysis, J. Phys. Chem. B 118 (2014) 3498–3506.
[117] H. Shi, N. Atlasevich, S.I. Merenbloom, D.E. Clemmer, Solution dependence of the collisional activation of ubiquitin [M+7H](7+) ions, J. Am. Soc. Mass Spectrom. 25 (2014) 2000–2008.
[118] N.A. Pierson, L. Chen, S.J. Valentine, D.H. Russell, D.E. Clemmer, Number of solution states of bradykinin from ion mobility and mass spectrometry measurements, J. Am. Chem. Soc. 133 (2011) 13810–13813.
[119] T. Wyttenbach, M.T. Bowers, Structural stability from solution to the gas phase: native solution structure of ubiquitin survives analysis in a solvent-free ion mobility-mass spectrometry environment, J. Phys. Chem. B 115 (2011) 12266–12275.
[120] H. Shi, N.A. Pierson, S.J. Valentine, D.E. Clemmer, Conformation types of ubiquitin $[M+8H]^{8+}$ ions from water:methanol solutions: evidence for the N and A states in aqueous solution, J. Phys. Chem. B 116 (2012) 3344–3352.
[121] A.E. Counterman, D.E. Clemmer, Anhydrous polyproline helices and globules, J. Phys. Chem. B 108 (2004) 4885–4898.
[122] K.B. Shelimov, M.F. Jarrold, "Denaturation" and refolding of cytochrome c in vacuo, J. Am. Chem. Soc. 118 (1996) 10313–10314.
[123] D.E. Clemmer, R.R. Hudgins, M.F. Jarrold, Naked protein conformations: cytochrome *c* in the gas-phase, J. Am. Chem. Soc. 117 (1995) 10141–10142.
[124] J.B. Fenn, Electrospray wings for molecular elephants (nobel lecture), Angew. Chem. Int. Ed. Engl. 42 (2003) 3871–3894.
[125] M.W. Zhou, V.H. Wysocki, Surface induced dissociation: dissecting noncovalent protein complexes in the gas phase, Acc. Chem. Res. 47 (2014) 1010–1018.
[126] F. Sobott, C.V. Robinson, Understanding protein interactions and their representation in the gas phase of the mass spectrometer, in: J. Laskin, C. Lifshitz (Eds.), Principles of Mass Spectrometry Applied to Biomolecules, John Wiley & Sons, Inc., Hoboken, NJ, USA, 2006.
[127] J.C. May, D.H. Russell, A mass-selective variable-temperature drift tube ion mobility-mass spectrometer for temperature dependent ion mobility studies, J. Am. Soc. Mass Spectrom. 22 (2011) 1134–1145.
[128] J.A. Silveira, K.L. Fort, D. Kim, K.A. Servage, N.A. Pierson, D.E. Clemmer, D.H. Russell, From solution to the gas phase: stepwise dehydration and kinetic trapping of substance P reveals the origin of peptide conformations, J. Am. Chem. Soc. 135 (2013) 19147–19153.
[129] J.A. Silveira, K.A. Servage, C.M. Gamage, D.H. Russell, Cryogenic ion mobility-mass spectrometry captures hydrated ions produced during electrospray ionization, J. Phys. Chem. A 117 (2013) 953–961.
[130] K.A. Servage, J.A. Silveira, K.L. Fort, D.H. Russell, Evolution of hydrogen-bond networks in protonated water clusters $H^+(H_2O)_n$ (n=1 to 120) studied by cryogenic ion mobility-mass spectrometry, J. Phys. Chem. Lett. 5 (2014) 1825–1830.
[131] K.A. Servage, J.A. Silveira, K.L. Fort, D.H. Russell, From solution to gas phase: the implications of intramolecular interactions on the evaporative dynamics of substance P during electrospray ionization, J. Phys. Chem. B 119 (2015) 4693–4698.
[132] E.R. Badman, C.S. Hoaglund-Hyzer, D.E. Clemmer, Monitoring structural changes of proteins in an ion trap over ~10–200 ms: unfolding transitions in cytochrome *c* ions, Anal. Chem. 73 (2001) 6000–6007.

[133] S. Lee, M.A. Ewing, F.M. Nachtigall, R.T. Kurulugama, S.J. Valentine, D.E. Clemmer, Determination of cross sections by overtone mobility spectrometry: evidence for loss of unstable structures at higher overtones, J. Phys. Chem. B 114 (2010) 12406–12415.
[134] B.T. Ruotolo, J.A. McLean, K.J. Gillig, D.H. Russell, Peak capacity of ion mobility mass spectrometry: the utility of varying drift gas polarizability for the separation of tryptic peptides, J. Mass Spectrom. 39 (2004) 361–367.
[135] A.E. Counterman, S.J. Valentine, C.A. Srebalus, S.C. Henderson, C.S. Hoaglund, D.E. Clemmer, High-order structure and dissociation of gaseous peptide aggregates that are hidden in mass spectra, J. Am. Soc. Mass Spectrom. 9 (1998) 743–759.
[136] R.S. Glaskin, M.A. Ewing, D.E. Clemmer, Ion trapping for ion mobility spectrometry measurements in a cyclical drift tube, Anal. Chem. 85 (2013) 7003–7008.
[137] A.A. Shvartsburg, Ultrahigh-resolution differential ion mobility separations of conformers for proteins above 10 kDa: onset of dipole alignment? Anal. Chem. 86 (2014) 10608–10615.
[138] J.A. Silveira, K. Michelmann, M.E. Ridgeway, M.A. Park, Path to resolving power beyond 250: a comprehensive trapped ion mobility spectrometry analytical model, in: 63rd ASMS Conference on Mass Spectrometry Allied Topics, St. Louis, MO, 2015.
[139] K. Giles, J.L. Wildgoose, S. Pringle, D. Langridge, P. Nixon, J. Garside, P. Carney, Characterising a T-wave enabled multi-pass cyclic ion mobility separator, in: 63rd ASMS Conference on Mass Spectrometry and Allied Topics, 2015.
[140] M. Groessl, S. Graf, M. Lisa, M. Holcapek, J. Sampaio, B. Dick, B. Vogt, R. Knochenmuss, Analysis of isomeric lipids by high resolution ion mobility-mass spectrometry, in: 63rd ASMS Conference on Mass Spectrometry and Allied Topics, 2015.
[141] J.C. Silva, R. Denny, C.A. Dorschel, M. Gorenstein, I.J. Kass, G.Z. Li, T. McKenna, M.J. Nold, K. Richardson, P. Young, S. Geromanos, Quantitative proteomic analysis by accurate mass retention time pairs, Anal. Chem. 77 (2005) 2187–2200.
[142] S.L. Koeniger, S.I. Merenbloom, S.J. Valentine, M.F. Jarrold, H.R. Udseth, R.D. Smith, D.E. Clemmer, An IMS–IMS analogue of MS–MS, Anal. Chem. 78 (2006) 4161–4174.
[143] S.C. Henderson, S.J. Valentine, A.E. Counterman, D.E. Clemmer, ESI/ion trap/ion mobility/time-of-flight mass spectrometry for rapid and sensitive analysis of biomolecular mixtures, Anal. Chem. 71 (1999) 291–301.
[144] J.A. McLean, B.T. Ruotolo, K.J. Gillig, D.H. Russell, Ion mobility-mass spectrometry: a new paradigm for proteomics, Int. J. Mass Spectrom. 240 (2005) 301–315.
[145] C.S. Hoaglund, S.J. Valentine, D.E. Clemmer, An ion trap interface for ESI-ion mobility experiments, Anal. Chem. 69 (1997) 4156–4161.
[146] K. Tang, A.A. Shvartsburg, H.N. Lee, D.C. Prior, M.A. Buschbach, F.M. Li, A.V. Tolmachev, G.A. Anderson, R.D. Smith, High-sensitivity ion mobility spectrometry/mass spectrometry using electrodynamic ion funnel interfaces, Anal. Chem. 77 (2005) 3330–3339.
[147] E.S. Baker, B.H. Clowers, F. Li, K. Tang, A.V. Tolmachev, D.C. Prior, M.E. Belov, R.D. Smith, Ion mobility spectrometry–mass spectrometry performance using electrodynamic ion funnels and elevated drift gas pressures, J. Am. Soc. Mass Spectrom. 18 (2007) 1176–1187.
[148] B.H. Clowers, Y.M. Ibrahim, D.C. Prior, W.F. Danielson III, M.E. Belov, R.D. Smith, Enhanced ion utilization efficiency using an electrodynamic ion funnel trap as an injection mechanism for ion mobility spectrometry, Anal. Chem. 80 (2008) 612–623.
[149] Y.M. Ibrahim, S.V.B. Garimella, A.V. Tolmachev, E.S. Baker, R.D. Smith, Improving ion mobility measurement sensitivity by utilizing helium in an ion funnel trap, Anal. Chem. 86 (2014) 5295–5299.
[150] A.V. Tolmachev, B.H. Clowers, M.E. Belov, R.D. Smith, Coulombic effects in ion mobility spectrometry, Anal. Chem. 81 (2009) 4778–4787.
[151] Y.M. Ibrahim, S.V. Garimella, A.V. Tolmachev, E.S. Baker, R.D. Smith, Improving ion mobility measurement sensitivity by utilizing helium in an ion funnel trap, Anal. Chem. 86 (2014) 5295–5299.
[152] I.K. Webb, S.V.B. Garimella, A.V. Tolmachev, T.-C. Chen, X. Zhang, J.T. Cox, R.V. Norheim, S.A. Prost, B. LaMarche, G.A. Anderson, Y.M. Ibrahim, R.D. Smith, Mobility-resolved ion selection in uniform drift field ion mobility spectrometry/mass spectrometry: dynamic switching in structures for lossless ion manipulations, Anal. Chem. 86 (2014) 9632–9637.
[153] I.K. Webb, S.V.B. Garimella, A.V. Tolmachev, T.C. Chen, X.Y. Zhang, R.V. Norheim, S.A. Prost, B. LaMarche, G.A. Anderson, Y.M. Ibrahim, R.D. Smith, Experimental evaluation and optimization of structures for loss less ion manipulations for ion mobility spectrometry with time-of-flight mass spectrometry, Anal. Chem. 86 (2014) 9169–9176.
[154] S.V. Garimella, Y.M. Ibrahim, I.K. Webb, A.V. Tolmachev, X. Zhang, S.A. Prost, G.A. Anderson, R.D. Smith, Simulation of electric potentials and ion motion in planar electrode structures for lossless ion manipulations (SLIM), J. Am. Soc. Mass Spectrom. 25 (2014) 1890–1896.
[155] T.-C. Chen, I.K. Webb, S.A. Prost, M.B. Harrer, R.V. Norheim, K. Tang, Y.M. Ibrahim, R.D. Smith, Rectangular ion funnel: a new ion funnel interface for structures for loss less ion manipulations, Anal. Chem. 87 (2015) 716–722.
[156] K.J. Gillig, B.T. Ruotolo, E.G. Stone, D.H. Russell, An electrostatic focusing ion guide for ion mobility-mass spectrometry, Int. J. Mass Spectrom. 239 (2004) 43–49.
[157] J.A. Silveira, C.M. Gamage, R.C. Blase, D.H. Russell, Gas-phase ion dynamics in a periodic-focusing DC ion guide, Int. J. Mass Spectrom. 296 (2010) 36–42.
[158] C.M. Gamage, J.A. Silveira, R.C. Blase, D.H. Russell, Gas-phase ion dynamics in a periodic-focusing DC ion guide (Part II): Discrete transport modes, Int. J. Mass Spectrom. 303 (2011) 154–163.
[159] J.A. Silveira, J. Jeon, C.M. Gamage, P.-J. Pai, K.L. Fort, D.H. Russell, Damping factor links periodic focusing and uniform field ion mobility for accurate determination of collision cross sections, Anal. Chem. 84 (2012) 2818–2824.
[160] K.L. Fort, J.A. Silveira, D.H. Russell, The periodic focusing ion funnel: theory, design, and experimental characterization by high-resolution ion mobility-mass spectrometry, Anal. Chem. 85 (2013) 9543–9548.
[161] E.R. Badman, S. Myung, D.E. Clemmer, Gas-phase separations of protein and peptide ion fragments generated by collision-induced dissociation in an ion trap, Anal. Chem. 74 (2002) 4889–4894.
[162] S.J. Valentine, D.E. Clemmer, H/D exchange levels of shape-resolved cytochrome c conformers in the gas phase, J. Am. Chem. Soc. 119 (1997) 3558–3566.
[163] M.F. Jarrold, E.C. Honea, Annealing of silicon clusters, J. Am. Chem. Soc. 114 (1992) 459–464.
[164] N.A. Pierson, S.J. Valentine, D.E. Clemmer, Evidence for a quasi-equilibrium distribution of states for bradykinin $[M+3H]^{3+}$ ions in the gas phase, J. Phys. Chem. B 114 (2010) 7777–7783.
[165] S.D. Pringle, K. Giles, J.L. Wildgoose, J.P. Williams, S.E. Slade, K. Thalassinos, R.H. Bateman, M.T. Bowers, J.H. Scrivens, An investigation of the mobility separation of some peptide and protein ions using a new hybrid quadrupole/travelling wave IMS/oa-ToF instrument, Int. J. Mass Spectrom. 261 (2007) 1–12.
[166] A.A. Shvartsburg, R.D. Smith, Fundamentals of traveling wave ion mobility spectrometry, Anal. Chem. 80 (2008) 9689–9699.
[167] K.D. Rand, S.D. Pringle, M. Morris, J.R. Engen, J.M. Brown, ETD in a traveling wave ion guide at tuned Z-spray ion source conditions allows for site-specific hydrogen/deuterium exchange measurements, J. Am. Soc. Mass Spectrom. 22 (2011) 1784–1793.
[168] I. Michaelevski, M. Eisenstein, M. Sharon, Gas-phase compaction and unfolding of protein structures, Anal. Chem. 82 (2010) 9484–9491.
[169] D. Morsa, V. Gabelica, E. De Pauw, Effective temperature of ions in traveling wave ion mobility spectrometry, Anal. Chem. 83 (2011) 5775–5782.
[170] S.I. Merenbloom, T.G. Flick, E.R. Williams, How hot are your ions in TWAVE ion mobility spectrometry? J. Am. Soc. Mass Spectrom. 23 (2012) 553–562.
[171] S.I. Merenbloom, S.L. Koeniger, S.J. Valentine, M.D. Plasencia, D.E. Clemmer, IMS–IMS and IMS–IMS–IMS/MS for separating peptide and protein fragment ions, Anal. Chem. 78 (2006) 2802–2809.
[172] S.I. Merenbloom, S.L. Koeniger, B.C. Bohrer, S.J. Valentine, D.E. Clemmer, Improving the efficiency of IMS–IMS by a combing technique, Anal. Chem. 80 (2008) 1918–1927.
[173] N.A. Pierson, D.E. Clemmer, An IMS–IMS threshold method for semi-quantitative determination of activation barriers: interconversion of proline cis↔trans forms in triply protonated bradykinin, Int. J. Mass Spectrom. 377 (2015) 646–654.
[174] G. Vidal-de-Miguel, M. Macía, C. Barrios, J. Cuevas, Transversal modulation ion mobility spectrometry (IMS) coupled with mass spectrometry (MS): exploring the IMS–IMS–MS possibilities of the instrument, Anal. Chem. 87 (2015) 1925–1932.
[175] A.V. Loboda, Setup for Mobility Separation of Ions Implementing an Ion Guide with an Axial Field and Counterflow of Gas, U.S. PTO, 2002.
[176] A. Loboda, Novel ion mobility setup combined with collision cell and time-of-flight mass spectrometer, J. Am. Soc. Mass Spectrom. 17 (2006) 691–699.
[177] K. Michelmann, J.A. Silveira, M.E. Ridgeway, M.A. Park, Fundamentals of trapped ion mobility spectrometry, J. Am. Soc. Mass Spectrom. 26 (2015) 14–24.
[178] D.R. Hernandez, J.D. DeBord, M.E. Ridgeway, D.A. Kaplan, M.A. Park, F. Fernandez-Lima, Ion dynamics in a trapped ion mobility spectrometer, Analyst 139 (2014) 1913–1921.
[179] J.A. Silveira, M.E. Ridgeway, M.A. Park, High resolution trapped ion mobility spectrometry of peptides, Anal. Chem. 86 (2014) 5624–5627.
[180] Y. Ibrahim, M.E. Belov, A.V. Tolmachev, D.C. Prior, R.D. Smith, Ion funnel trap interface for orthogonal time-of-flight mass spectrometry, Anal. Chem. 79 (2007) 7845–7852.
[181] M.E. Ridgeway, J. Silveira, J. Meier, M.A. Park, Parallel ion accumulation and analysis for 100% duty cycle in trapped ion mobility spectrometry, in: 63rd ASMS Conference on Mass Spectrometry Allied Topics, St. Louis, MO, 2015.
[182] M.E. Ridgeway, J.A. Silveira, J.E. Meier, M.A. Park, Microheterogeneity within conformational states of ubiquitin revealed by high resolution trapped ion mobility spectrometry, Analyst 140 (2015) 6964–6972.
[183] P. Benigni, C.J. Thompson, M.E. Ridgeway, M.A. Park, F. Fernandez-Lima, Targeted high-resolution ion mobility separation coupled to ultrahigh-resolution mass spectrometry of endocrine disruptors in complex mixtures, Anal. Chem. 87 (2015) 4321–4325.
[184] J.D. Canterbury, X. Yi, M.R. Hoopmann, M.J. MacCoss, Assessing the dynamic range and peak capacity of nanoflow LC–FAIMS–MS on an ion trap mass spectrometer for proteomics, Anal. Chem. 80 (2008) 6888–6897.
[185] J. Saba, E. Bonneil, C. Pomies, K. Eng, P. Thibault, Enhanced sensitivity in proteomics experiments using FAIMS coupled with a hybrid linear ion trap/orbitrap mass spectrometer, J. Proteome Res. 8 (2009) 3355–3366.
[186] S.M. Zucker, S. Lee, N. Webber, S.J. Valentine, J.P. Reilly, D.E. Clemmer, An ion mobility/ion trap/photodissociation instrument for characterization of ion structure, J. Am. Soc. Mass Spectrom. 22 (2011) 1477–1485.

[187] E.W. Robinson, D.E. Garcia, R.D. Leib, E.R. Williams, Enhanced mixture analysis of poly(ethylene glycol) using high-field asymmetric waveform ion mobility spectrometry combined with Fourier transform ion cyclotron resonance mass spectrometry, Anal. Chem. 78 (2006) 2190–2198.
[188] V. Frankevich, P.M.-L. Sinues, K. Barylyuk, R. Zenobi, Ion mobility spectrometry coupled to laser-induced fluorescence, Anal. Chem. 85 (2013) 39–43.
[189] W. Schrader, Y. Xuan, A. Gaspar, Studying ultra-complex crude oil mixtures by using high-field asymmetric waveform ion mobility spectrometry (FAIMS) coupled to an electrospray ionisation-LTQ-Orbitrap mass spectrometer, Eur. J. Mass Spectrom. 20 (2014) 43–49.
[190] R.W. Purves, R. Guevremont, Electrospray ionization high-field asymmetric waveform ion mobility spectrometry–mass spectrometry, Anal. Chem. 717 (1999) 2346–2357.
[191] G. Papadopoulos, A. Svendsen, O.V. Boyarkin, T.R. Rizzo, Spectroscopy of mobility-selected biomolecular ions, Faraday Discuss. 150 (2011) 243–255.
[192] M. Cui, L.Y. Ding, Z. Mester, Separation of cisplatin and its hydrolysis products using electrospray ionization high-field asymmetric waveform ion mobility spectrometry coupled with ion trap mass spectrometry, Anal. Chem. 75 (2003) 5847–5853.
[193] M.F. Jarrold, J.E. Bower, K. Creegan, Chemistry of semiconductor clusters: a study of the reactions of size selected Si_n^+ (n = 3–24) with C_2H_4 using selected ion drift tube techniques, J. Chem. Phys. 90 (1989) 3615–3628.
[194] P. Dugourd, R.R. Hudgins, D.E. Clemmer, M.F. Jarrold, High-resolution ion mobility measurements, Rev. Sci. Instrum. 68 (1997) 1122–1129.
[195] A.C. Gill, K.R. Jennings, T. Wyttenbach, M.T. Bowers, Conformations of biopolymers in the gas phase: a new mass spectrometric method, Int. J. Mass Spectrom. 195 (2000) 685–697.
[196] P.R. Kemper, M.T. Bowers, A hybrid double-focusing mass-spectrometer – high-pressure drift reaction cell to study thermal-energy reactions of mass-selected ions, J. Am. Soc. Mass Spectrom. 1 (1990) 197–207.
[197] J.S. Page, I. Marginean, E.S. Baker, R.T. Kelly, K. Tang, R.D. Smith, Biases in ion transmission through an electrospray ionization-mass spectrometry capillary inlet, J. Am. Soc. Mass Spectrom. 20 (2009) 2265–2272.
[198] F.J. Knorr, R.L. Eatherton, W.F. Siems, H.H. Hill, Fourier-transform ion mobility spectrometry, Anal. Chem. 57 (1985) 402–406.
[199] B.H. Clowers, A. Davis, K. Morrison, W.F. Siems, Reviving the Fourier transform to characterize gasphase intermediates in ion mobility-mass spectrometry experiments, in: 63rd ASMS Conference on Mass Spectrometry and Allied Topics, St. Louis, MO, 2015.
[200] A.W. Szumlas, G.M. Hieftje, Phase-resolved detection in ion-mobility spectrometry, Anal. Chim. Acta 566 (2006) 45–54.
[201] A.W. Szumlas, S.J. Ray, G.M. Hieftje, Hadamard transform ion mobility spectrometry, Anal. Chem. 78 (2006) 4474–4481.
[202] M.E. Belov, M.A. Buschbach, D.C. Prior, K.Q. Tang, R.D. Smith, Multiplexed ion mobility spectrometry–orthogonal time-of-flight mass spectrometry, Anal. Chem. 79 (2007) 2451–2462.
[203] B.H. Clowers, M.E. Belov, D.C. Prior, W.F. Danielson III, Y. Ibrahim, R.D. Smith, Pseudorandom sequence modifications for ion mobility orthogonal time-of-flight mass spectrometry, Anal. Chem. 80 (2008) 2464–2473.
[204] M. Belov, W. Danielson, D. Goodlett, Bridging the gap between ion mobility spectrometry and an orbitrap, in: 63rd ASMS Conference on Mass Spectrometry and Allied Topics, St. Louis, MO, 2015.
[205] S.L. Kaufman, Analysis of biomolecules using electrospray and nanoparticle methods: the gas-phase electrophoretic mobility molecular analyzer (GEMMA), J. Aerosol Sci. 29 (1998) 537–552.
[206] P. Martinez-Lozano, E. Criado, G. Vidal, S. Cristoni, F. Franzoso, M. Piatti, P. Brambilla, Differential mobility analysis-mass spectrometry coupled to XCMS algorithm as a novel analytical platform for metabolic profiling, Metabolomics 9 (2013) S30–S43.
[207] H. Ouyang, C. Larriba-Andaluz, D.R. Oberreit, C.J. Hogan, The collision cross sections of iodide salt cluster ions in air via differential mobility analysis-mass spectrometry, J. Am. Soc. Mass Spectrom. 24 (2013) 1833–1847.
[208] B.B. Schneider, E.G. Nazarov, F. Londry, P. Vouros, T.R. Covey, Differential mobility spectrometry/mass spectrometry history, theory, design optimization, simulations, and applications, Mass Spectrom. Rev. (2015), http://dx.doi.org/10.1002/mas.21453.
[209] G.A. Eiceman, E.V. Krylov, B. Tadjikov, R.G. Ewing, E.G. Nazarov, R.A. Miller, Differential mobility spectrometry of chlorocarbons with a micro-fabricated drift tube, Analyst 129 (2004) 297–304.
[210] R. Guevremont, R.W. Purves, D.A. Barnett, L.Y. Ding, Ion trapping at atmospheric pressure (760 Torr) and room temperature with a high-field asymmetric waveform ion mobility spectrometer, Int. J. Mass Spectrom. 193 (1999) 45–56.
[211] R. Guevremont, R.W. Purves, Atmospheric pressure ion focusing in a high-field asymmetric waveform ion mobility spectrometer, Rev. Sci. Instrum. 70 (1999) 1370–1383.
[212] D.A. Barnett, R.W. Purves, R. Guevremont, Isotope separation using high-field asymmetric waveform ion mobility spectrometry, Nucl. Instrum. Methods Phys. Res. A 450 (2000) 179–185.
[213] R. Guevremont, L. Ding, B. Ells, D.A. Barnett, R.W. Purves, Atmospheric pressure ion trapping in a tandem FAIMS–FAIMS coupled to a TOFMS: studies with electrospray generated gramicidin S ions, J. Am. Soc. Mass Spectrom. 12 (2001) 1320–1330.
[214] D.A. Barnett, L. Ding, B. Ells, R.W. Purves, R. Guevremont, Tandem mass spectra of tryptic peptides at signal-to-background ratios approaching unity using electrospray ionization high-field asymmetric waveform ion mobility spectrometry/hybrid quadrupole time-of-flight mass spectrometry, Rapid Commun. Mass Spectrom. 16 (2002) 676–680.
[215] A.A. Shvartsburg, D.E. Clemmer, R.D. Smith, Isotopic effect on ion mobility and separation of isotopomers by high-field ion mobility spectrometry, Anal. Chem. 82 (2010) 8047–8051.
[216] A.A. Shvartsburg, T.A. Seim, W.F. Danielson, R. Norheim, R.J. Moore, G.A. Anderson, R.D. Smith, High-definition differential ion mobility spectrometry with resolving power up to 500, J. Am. Soc. Mass Spectrom. 24 (2013) 109–114.
[217] A.A. Shvartsburg, S.V. Mashkevich, R.D. Smith, Feasibility of higher-order differential ion mobility separations using new asymmetric waveforms, J. Phys. Chem. A 110 (2006) 2663–2673.
[218] A.B. Hall, S.L. Coy, A. Kafle, J. Glick, E. Nazarov, P. Vouros, Extending the dynamic range of the ion trap by differential mobility filtration, J. Am. Soc. Mass Spectrom. 24 (2013) 1428–1436.
[219] M.J. Kailemia, M. Park, D.A. Kaplan, A. Venot, G.J. Boons, L.Y. Li, R.J. Linhardt, I.J. Amster, High-field asymmetric-waveform ion mobility spectrometry and electron detachment dissociation of isobaric mixtures of glycosaminoglycans, J. Am. Soc. Mass Spectrom. 25 (2014) 258–268.
[220] S.J. Valentine, R.T. Kurulugama, D.E. Clemmer, Overtone mobility spectrometry: Part 3. On the origin of peaks, J. Am. Soc. Mass Spectrom. 22 (2011) 804–816.
[221] M.A. Ewing, S.M. Zucker, S.J. Valentine, D.E. Clemmer, Overtone mobility spectrometry: Part 5. Simulations and analytical expressions describing overtone limits, J. Am. Soc. Mass Spectrom. 24 (2013) 615–621.
[222] M.A. Ewing, C.R. Conant, S.M. Zucker, K.J. Griffith, D.E. Clemmer, Selected overtone mobility spectrometry, Anal. Chem. 87 (2015) 5132–5138.
[223] R.S. Glaskin, S.J. Valentine, D.E. Clemmer, A scanning frequency mode for ion cyclotron mobility spectrometry, Anal. Chem. 82 (2010) 8266–8271.
[224] K. Giles, J. Wildgoose, S.D. Pringle, J. Garside, P. Carney, P. Nixon, D.J. Langridge, Design and utility of a multi-pass cyclic ion mobility separator, in: 62nd Annual ASMS Conference on Mass Spectrometry and Allied Topics, Baltimore, MD, 2014.
[225] R.S. Glaskin, New Techniques for High Mobility Resolution and Ion Dynamics in a Circular Drift Tube, Chemistry Indiana University, UMI Dissertations Publishing, 2013, pp. 192.
[226] G. Vidal-de-Miguel, in: USPTO (Ed.), Method and Apparatus to Produce Steady Beams of Mobility Selected Ions via Time-dependent Electric Fields, USPTO, Sociedad Europea de Analisis Diferencial de Movilidad, USA, 2013.
[227] C. Barrios-Collado, G. Vidal-de-Miguel, Numerical algorithm for the accurate evaluation of ion beams in transversal modulation ion mobility spectrometry: understanding realistic geometries, Int. J. Mass Spectrom. 376 (2015) 97–105.
[228] P.M. Lalli, B.A. Iglesias, H.E. Toma, G.F. de Sa, R.J. Daroda, J.C. Silva Filho, J.E. Szulejko, K. Araki, M.N. Eberlin, Protomers: formation, separation and characterization via travelling wave ion mobility mass spectrometry, J. Mass Spectrom. 47 (2012) 712–719.
[229] S.J. Valentine, D.E. Clemmer, Treatise on the measurement of molecular masses with ion mobility spectrometry, Anal. Chem. 81 (2009) 5876–5880.
[230] R.T. Kurulugama, F.M. Nachtigall, S.J. Valentine, D.E. Clemmer, Overtone mobility spectrometry: Part 4. OMS-OMS analyses of complex mixtures, J. Am. Soc. Mass Spectrom. 22 (2011) 2049–2060.